Published for SISSA by Springer

Received: *September 5, 2011*
Accepted: *October 7, 2011*
Published: *November 8, 2011*

Small hairy black holes in $AdS_5 \times S^5$

Sayantani Bhattacharyya,[a] **Shiraz Minwalla**[a] **and Kyriakos Papadodimas**[b]

[a] *Tata Institute of Fundamental Research, Homi Bhabha Rd, Mumbai 400005, India*
[b] *Institute for Theoretical Physics, Valckenierstraat 65, 1018 XE Amsterdam, The Netherlands*

E-mail: sayanta@theory.tifr.res.in, minwalla@theory.tifr.res.in, k.papadodimas@uva.nl

Abstract: We study small hairy black holes in a consistent truncation of $\mathcal{N} = 8$ gauged supergravity that consists of a single charged scalar field interacting with the metric and a U(1) gauge field. Small very near extremal RNAdS black holes in this system are unstable to decay by superradiant emission. The end point of this instability is a small hairy black hole that we construct analytically in a perturbative expansion in its charge. Unlike their RNAdS counterparts, hairy black hole solutions exist all the way down to the BPS bound, demonstrating that $\mathcal{N} = 4$ Yang Mills theory has an $\mathcal{O}(N^2)$ entropy at all energies above supersymmetry. At the BPS bound these black holes reduce to previously discussed regular, supersymmetric horizon free solitons. We use numerical methods to continue the construction of these solitons to large charges and find that the line of soliton solutions terminates at a singular solution S at a finite charge. We conjecture that a one parameter family of singular supersymmetric solutions, which emerges out of S, constitutes the BPS limit of hairy black holes at larger values of the charge. We analytically determine the near singularity behaviour of S, demonstrate that both the regular and singular solutions exhibit an infinite set of damped 'self similar' oscillations around S and analytically compute the frequency of these oscillations. At leading order in their charge, the thermodynamics of the small hairy black holes constructed in this paper turns out to be correctly reproduced by modeling these objects as a non interacting mix of an RNAdS black hole and the supersymmetric soliton in thermal equilibrium. Assuming that a similar non interacting model continues to apply upon turning on angular momentum, we also predict a rich family of rotating hairy black holes, including new hairy supersymmetric black holes. This analysis suggests interesting structure for the space of (yet to be constructed) hairy charged rotating black holes in $AdS_5 \times S^5$, particularly in the near BPS limit.

Keywords: Gauge-gravity correspondence, AdS-CFT Correspondence, Black Holes

ArXiv ePrint: 1005.1287

doi:10.1007/JHEP11(2011)035

JHEP11(2011)035

Contents

JHEP11(2011)035

JHEP11(2011)035

1 Introduction

Black hole solutions of IIB theory on $AdS_5 \times S^5$ constitute the thermodynamic saddle points of $\mathcal{N} = 4$ Yang Mills theory on S^3 via the AdS/CFT correspondence. A complete understanding of the space of stationary black hole solutions in $AdS_5 \times S^5$ is consequently essential for a satisfactory understanding of the state space of $\mathcal{N} = 4$ Yang Mills theory at energies of order N^2. While the Kerr RNAdS black hole solutions are well known [1–7], it seems likely that several additional yet to be determined families of black hole solutions will play an important role in the dynamics and thermodynamics of $\mathcal{N} = 4$ Yang Mills theory.

In this paper we will construct a new class of asymptotically $AdS_5 \times S^5$ black hole solutions. The black holes we construct are small, charged, and have parametrically low temperatures; our construction is perturbative in the black hole charge. Our solutions are hairy, in the sense that they include condensates of charged scalar fields.[1] In the BPS limit these hairy black holes reduce to regular horizon free solitons. We also use numerical techniques to continue our perturbative construction of these solitons to charges of order unity, and uncover an intricate self similar behaviour in the space of solitons in the neighborhood of a finite critical value of the charge. The solutions presented in this paper suggest a qualitatively new picture of the near BPS spectrum of $\mathcal{N} = 4$ Yang Mills.

Our perturbative construction of hairy black holes is close in spirit and technique to the constructions presented in the recent paper [14], which may be regarded as an immediate precursor to the current work. For this reason we first present a brief review of [14] before turning to a description and discussions of the new black hole solutions constructed in this paper.

[1] See [8–12] and references therein for reviews of recent work — sparked by an observation by Gubser [13] — on hairy black branes in AdS spaces.

It was demonstrated in [14] that small charged black holes in global AdS spaces are sometimes unstable to the condensation of charged matter fields. More precisely any system governed by the Lagrangian

$$\int d^5x\sqrt{g}\left[\frac{1}{2}(R+12)-\frac{3}{8}F_{\mu\nu}F^{\mu\nu}-\frac{3}{16}\left(|D_\mu\phi|^2+\Delta(\Delta-4)\phi\phi^*\right)+\text{Interactions}\right] \tag{1.1}$$
$$D_\mu\phi=\partial_\mu\phi-eiA_\mu\phi$$

possesses small RNAdS black holes that are unstable to decay by superradiant discharge of the scalar field ϕ whenever $e>\Delta$. The end point of this superradiant tachyon condensation process is a hairy black hole. The authors of [14] constructed these hairy black hole solutions (working with a particular toy model Lagrangian of the form (1.1)) in a perturbation expansion in their mass and charge. At leading order in this expansion, the hairy black holes of [14] are well approximated by a non interacting mix of a small RNAdS black hole and a weak static solitonic scalar condensate. In particular, it was shown in [14] that the leading order thermodynamics of small hairy black holes could be reproduced simply by modeling them as a non interacting mix of an RNAdS black hole and a regular charged scalar soliton.

The results of [14] suggest that the density of states of certain field theories with a gravity dual description might be dominated in certain regimes by previously unexplored phases consisting of an approximately non interacting mix of a normal charged phase and a Bose condensate. In order to make definitive statements about the actual behaviour of $\mathcal{N}=4$ Yang Mills theory, however, it is necessary to perform the relevant calculations in IIB supergravity on $AdS_5\times S^5$ rather than a simple toy model Lagrangian; this is the subject of the current paper. As the IIB theory on $AdS_5\times S^5$ is a very special system, the reader might anticipate that hairy black holes in this theory have some distinctive special properties not shared by equivalent objects in the toy model studied in [14] at least at generic values of parameters. As we will see below, this indeed turns out to be the case.

In order to avoid having to deal with the full complexity of IIB SUGRA, in this paper we identify[2] work with a consistent truncation of gauged $\mathcal{N}=8$ supergravity (itself a consistent truncation of IIB SUGRA on $AdS_5\times S^5$). Of the complicated spectrum of $\mathcal{N}=8$ supergravity, our truncation retains only a single charged scalar field ϕ, a gauge field A_μ and the metric.[3] The Lagrangian for our system is given by

$$\begin{aligned}S=&\frac{N^2}{4\pi^2}\int\sqrt{g}\Big[\frac{1}{2}(R+12)-\frac{3}{8}F_{\mu\nu}F^{\mu\nu}-\frac{3}{16}\left(|D_\mu\phi|^2-\frac{\partial_\mu(\phi\phi^*)\partial^\mu(\phi\phi^*)}{4(4+\phi\phi^*)}-4\phi\phi^*\right)\\&+\frac{1}{8\sqrt{g}}\epsilon^{\alpha\beta\gamma\mu\nu}F_{\alpha\beta}F_{\gamma\mu}A_\nu\Big]\end{aligned} \tag{1.2}$$
$$D_\mu\phi=\partial_\mu\phi-2iA_\mu\phi$$
$$F_{\mu\nu}=\partial_\mu A_\nu-\partial_\nu A_\mu$$

[2] In unpublished work, S. Gubser, C. Herzog and S. Pufu have independently identified this consistent truncation, and have numerically investigated hairy black branes in this set up. We thank C. Herzog for informing us of this.

[3] Under the AdS/CFT correspondence, ϕ is dual to the operator $TrX^2+TrY^2+TrZ^2$ while A_μ is dual to the conserved current $J_\mu^{X\bar{X}}+J_\mu^{Y\bar{Y}}+J_\mu^{Z\bar{Z}}$. Here X, Y and Z denote the three complex chiral scalars in the $\mathcal{N}=4$ Lagrangian.

JHEP11(2011)035

and is of the general structure (1.1) with $e = 2$ and $\Delta = 2$. As $e = \Delta$, small very near extremal black holes in this system lie at the precipice of the super radiant instability discussed in [14]. The question of whether they fall over this precipice requires a detailed calculation. We perform the necessary computation in this paper. Our results demonstrate that very near extremal small black holes *do* suffer from the super radiant instability; we proceed to construct the hairy black hole that constitutes the end point of this instability.

The calculations presented in this paper employ techniques that are similar to those used in [14]. In particular we work in a perturbation expansion in the scalar amplitude using very near extremal vacuum RNAdS black holes as the starting point of our expansion. This expansion is justified by the smallness of the charge of our solutions. We implement our perturbative procedure by matching solutions in a near (horizon) range, intermediate range and far field range. This matching procedure is justified by the parametrically large separation of scales between the horizon radius of the black holes we construct and AdS curvature radius. We refer the reader to the introduction of [14] for a more detailed explanation of physical motivation for this perturbative expansion and its formal structure. Actual details of our calculations may be found in sections 3 and 4 below. In the rest of this introduction we simply present our results and comment on their significance.

We study black holes of charge Q[4] (normalized so that each of the three complex Yang Mills scalars has unit charge) and mass M (normalized to match the scaling dimensions of dual operators). We find it convenient to deal with the 'intensive' mass and charge, m and q, given by

$$m = \frac{M}{N^2} \quad q = \frac{Q}{N^2}.$$

As in [14], in this paper we are primarily interested in small black holes for which $q \ll 1$ and $m \ll 1$. We now recall some facts about RNAdS black holes in this system. First, the masses of such black holes obey the inequality

$$m \geq m_{ext}(q) = 3q + 3q^2 - 6q^3 + \mathcal{O}(q^4)$$

Black holes that saturate this inequality are extremal, regular and have finite entropy (see subsection 6.1 for more details). The chemical potential $\mu_{ext}(q)$ of extremal black holes is given by

$$\mu_{ext}(q) = 1 + 2q - 6q^2 + \mathcal{O}(q^3)$$

and approaches unity in the limit of small charge. Note also that extremal black holes lie above the BPS bound

$$m_{BPS}(q) = 3q$$

and in particular that $m_{ext}(q) - m_{BPS}(q) = 3q^2 + \mathcal{O}(q^3)$

We will now investigate potential superradiant instabilities (see the introduction of [14] for an explanation of this term) of these black holes. Recall that a mode of charge e and energy ω scatters off a black hole of chemical potential μ in a superradiant manner whenever $\mu e > \omega$. The various modes of the scalar field ϕ in (1.2) have energies $\omega = 2, 3, \ldots$ and

[4] Q is the charge of the black hole solutions under each of the three diagonal U(1) Cartan's of SO(6). The consistent truncation of this paper forces these three U(1) charges to be equal.

JHEP11(2011)035

all carry charge $e = 2$. As the chemical potential of a small near extremal black hole is approximately unity, it follows that only the ground state of ϕ (with $\omega = \Delta = 2$) could possibly scatter of a near extremal RNAdS black hole in a superradiant manner. This mode barely satisfies the condition for superradiant scattering; as a consequence we will show in this paper that small RNAdS black holes in (1.2) suffer from a superradiant instability into this ground state mode only very near to extremality, i.e. when

$$m - m_{ext}(q) \leq 6q^3 + \mathcal{O}(q^4).$$

Unstable black holes eventually settle down into a new branch of stable hairy black hole solutions. We have constructed these hairy black holes in a perturbative expansion in their charge in section 4; we now proceed to present a qualitative description of these solutions and their thermodynamics.

Recall that the zero mode of the scalar field ϕ obeys the BPS bound (and so is supersymmetric) at linear order in an expansion about global AdS_5. It has been demonstrated in [15–17] (and we reconfirm in section 3 below) that this linearized BPS solution continues into a nonlinear BPS solution upon increasing its amplitude. In this paper we will refer to this regular solution as the supersymmetric soliton. The hairy black holes of this paper may approximately be thought of as a small, very near extremal RNAdS black hole located in the center of one of these solitons. Although the soliton is supersymmetric, the black hole at its center is not, and so hairy black holes are not BPS in general. These solutions exist in the mass range

$$3q \leq m \leq 3q + 3q^2 + \mathcal{O}(q^4) \tag{1.3}$$

At the lower bound of this range (7.14) hairy black holes reduce to the supersymmetric soliton. At the upper bound (which is also the instability curve for RNAdS black holes) they reduce to RNAdS black holes.

In figure 1 below we have plotted the near extremal micro canonical 'phase diagram' for our system. As is apparent from figure 1 our system undergoes a phase transition from an RNAdS phase to a hairy black hole phase upon lowering the energy at fixed charge. This phase transition occurs at the upper end of the range (1.3). Note that the phase diagram of figure 1 has several similarities with the phase diagram depicted in figure 1 in [14]; however there is also one important difference. The temperature of the hairy black holes of this paper decreases with decreasing mass at fixed charge, and reaches the value zero at the BPS bound. In contrast the temperature of the hairy black holes of [14] increases with decreasing mass (at fixed charge), approaching infinity in the vicinity of the lower bound.

As we have emphasized, the phase diagram depicted in figure 1 applies only in the limit of small charges and masses. We would now like to inquire as to how this phase diagram continues to large charges and masses. In order to address this question we first focus on solitonic solutions. These solutions may be determined much more simply than the generic hairy solution, as they obey the constraints of supersymmetry rather than simply the equations of motion. It turns out that spherically symmetric supersymmetric solutions are given as solutions to a single nonlinear, second order ordinary differential equation [15–17]. The solitons constitute the unique one parameter set of regular solutions to this equation. It is easy to continue our perturbative construction of the solitonic

JHEP11(2011)035

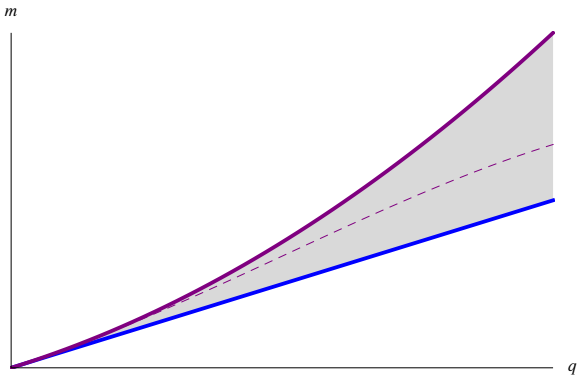

Figure 1. Phase diagram as a function of charge q (x axis) and mass m (y axis) at small q. The solid blue line at the bottom is the BPS bound along which the soliton lives. Hairy black holes exist — and are the dominant phase — in the shaded region. RNAdS black holes are the only known solutions (so in particular the dominant phase) in the unshaded region above the solid red curve at the top. RNAdS black holes also exist (but are dynamically unstable and thermodynamically sub dominant) between the solid red curve and the dashed curve. The solid red curve is described by $m = 3q + 3q^2 + \mathcal{O}(q^4)$, while the blue curve by $m = 3q$. The dashed curve corresponds to extremal RNAdS black holes and is given by $m = 3q + 3q^2 - 6q^3 + \mathcal{O}(q^4)$. The curves have not been drawn to scale to make the diagram more readable.

solutions to large charges by solving this equation numerically: in fact this exercise was already carried out in [16]. This numerical solution reveals that the solitonic branch of solutions terminates at a finite charge $q_c = 0.2613$. For $q > q_c$ there are no supersymmetric spherically symmetric solutions to the equations of motion of (1.2).[5]

Recall that solitons constitute the lower edge of the space of hairy black hole solutions of figure 1. The non existence of regular supersymmetric solutions for $q > q_c$ might, at first, suggest that at these charges the space of hairy black hole solutions terminates at a mass greater than $3q$ (i.e. does not extend all the way down to supersymmetry). While this is a logical possibility, we think it is likely that the truth lies elsewhere. As we will explain in section 5 the solitonic branch of supersymmetric solutions terminates in a distinguished singular solution S. It turns out that S is also the end point (or origin) of a one parameter set of supersymmetric solutions that are all singular at the origin. The charges of these solutions increase without bound (indeed we have found an explicit analytic solution for the singular supersymmetric solution in the limit of arbitrarily large charge). The two one parameter families of solutions, regular and singular ones, are joined at the special solution S. We conjecture that smooth hairy black hole solutions exist in our system at every q and for $m > 3q$. Upon taking the limit $m \to 3q$, these smooth solutions reduce to the smooth soliton for $q < q_c$ but reduce to the singular supersymmetric solutions described above when $q > q_c$. In summary, we conjecture that the phase diagram of our system takes the form displayed in figure 2 below.

[5]To be more precise, there are smooth solitonic solutions up to a slightly higher value $q_m = 0.2643$, but in a sense that will be explained in section 5, the point q_c marks the boundary between regular solitonic solutions and singular ones.

JHEP11(2011)035

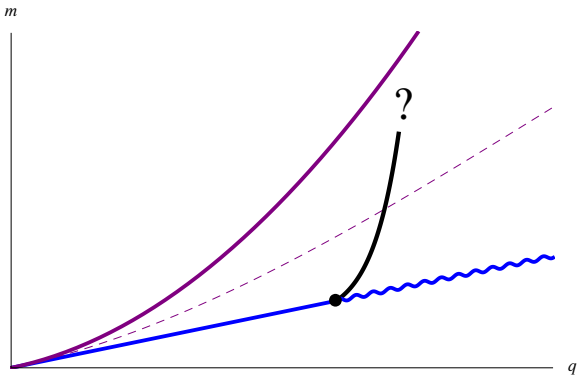

Figure 2. Conjectured phase diagram as a function of charge q (x axis) and mass m (y axis) for all values of q. The blue line at the bottom is the BPS bound along which the regular soliton lives (straight part) and the singular supersymmetric solutions (wiggly part). The solid red curve at the top marks the phase transition between the regime of RNAdS black holes (above the line) and that of smooth hairy black holes (below). The black curve indicates a phase transition between different types of hairy black holes. This curve originates from the BPS line at the black dot which is close to the point $q = q_c$ and could end either in the bulk of the hairy black hole region or could extend all the way up to the red line.

The distinguished solution S clearly plays a special role in the space of spherically symmetric supersymmetric solutions. In subsection 5.2 we analytically determine the near singularity behaviour of this solution. Viewing the 2nd order differential equation that determines supersymmetric solutions as a dynamical system in the 'time' variable $\ln r$, we demonstrate that the solution S is a stable fixed point of this system, and analytically compute the eigenvalues that characterize the approach to this fixed point. This eigenvalue has an imaginary part (which damps fluctuations) and a real part (that results in oscillations). Solitonic — and singular — solutions in the neighborhood of S may be thought of as configurations that that flow to S at large $\ln r$. The oscillations[6] referred to above result in the following phenomenon: the system develops a multiplicity of supersymmetric solitonic (or singular) at charges q when q comes near enough to q_c. The number of solutions diverges as $q \to q_c$. The space of solitonic and singular supersymmetric solutions are usefully plotted as a curve on a plane parametrized by the charge q and the expectation value of the operator dual to the scalar ϕ. On this plane supersymmetric solitons spiral into the point S, while the singular solutions spiral out of the same point (see figure 15); the two spirals are non self intersecting.[7] We find this extremely intricate structure of supersymmetric solutions quite fascinating, and feel that its implications for $\mathcal{N} = 4$ Yang Mills physics certainly merits further investigation.

In this paper we have so far only considered charged black holes with vanishing angular momentum. Such solutions are spherically symmetric; i.e. they preserve the SO(4) =

[6]We are extremely grateful to M. Rangamani for suggesting that we look for this 'self similar' structure in the space of solitons in the neighborhood of $q = q_c$. The results reported in this paragraph are the outcome of investigations that were spurred directly by this suggestion.

[7]We are very grateful to V. Hubeny for suggesting the possibility of a spiral structure for these curves.

JHEP11(2011)035

SU(2) × SU(2) rotational isometry group. As all known supersymmetric black holes in $AdS_5 \times S^5$ possess angular momentum [18–20], it is of interest to generalize the study of this paper to black holes with angular momentum. Let us first consider a spinning Kerr RNAdS black hole that preserves only U(1) × U(1) ∈ SU(2) × SU(2). Perturbations about such a solution are functions of an angle and a radius and are given by solutions to partial rather than ordinary differential equations. However there exist RNAdS black holes with self dual angular momentum. The angular momentum of such a black hole lie entirely within one of the two SU(2) above, and so preserve a U(1) × SU(2) subgroup of the rotation group. Perturbations around these solutions may be organized in representations of SU(2) and so obey ordinary rather than partial differential equations.[8] Consequently, the generalization of the hairy black hole solutions determined in this paper to solutions with self dual spin appears to be a plausibly tractable project; which we however leave to future work.

Even though we do not embark on a serious analysis of charged rotating black holes in this paper, we do present a speculative appetizer for this problem. In more detail we present a guess (or a prediction) for the leading order thermodynamics of these spinning hairy solutions. Our guess is based on the observation that the thermodynamics of the hairy solutions constructed in this paper can be reproduced, at leading order, by modeling the hairy black hole as a non interacting mix of a RNAdS black hole and the soliton. In section 7 we simply assume that a similar model works for charged spinning black holes, and use this model to compute the thermodynamics of a certain class of spinning hairy black holes. The most interesting aspect of our results concern the BPS limit. Our non interacting model predicts that extremal hairy black holes are BPS at every value of the angular momentum and charge. This is in stark contrast with Kerr RNAdS black holes that are BPS only on a co dimension one surface of the space of extremal black holes. According to our non interacting model, BPS hairy black holes are a non interacting mix of Gutowski Reall black holes [18–20] and supersymmetric solitons. Such a mix is thermally equlibrated at all values of charge and angular momentum because of an important property of Gutowski Reall black holes; their chemical potential is exactly unity.[9] We find this result both intriguing and puzzling (see e.g. [21]). We emphasize that our prediction is based on the non interacting superposition model, which may or may apply to actual black hole solutions. We leave further investigation of this extremely interesting issue to future work.

This paper has been devoted largely to the study of small very near extremal charged black holes in AdS_5 that are smeared over S^5. As uncharged small smeared black holes are well known to suffer from Gregory-Laflamme type instabilities [22], the reader may wonder whether the black holes studied in this paper might suffer from similar instabilities. We believe that this is not the case. Recall that the likely end point of a Gregory Laflamme type instability is a small black hole of proper horizon radius r_H localized on the S^5. In order that this black hole be near extremal, it has to zip around the S^5 at near the speed of light, i.e. at $v = 1 - \delta$ with $\delta \ll 1$. The AdS_5 charge of such a black hole is given by $q \propto \frac{r_H^7}{\sqrt{\delta}}$

[8] We thank A. Strominger for pointing this out to us.

[9] We are very grateful to S. Kim for explaining this to us.

JHEP11(2011)035

while its energy above extremality of such a black hole is given by $m - 3q \propto r_H^7 \sqrt{\delta}$.[10] We may now solve for r_H and δ as a function of q and $m-3q$. In the near BPS limit of interest to this paper $m - 3q \sim q^2$ and we find $r_H^7 \propto q^{\frac{3}{2}}$ and $\sqrt{\delta} \propto \sqrt{q}$. It follows that the entropy of such a localized black hole $\propto r_H^8 \propto q^{\frac{3}{2}\times\frac{8}{7}}$, and so is smaller than the entropy, $(\propto q^{\frac{3}{2}})$, of the black holes studied in this paper. As the the black holes studied in this paper have higher entropy than S^5 localized black holes with the same charge, there seems no reason to expect them to suffer from Gregory-Laflamme type instabilities.[11] Another pointer to the same conclusion is the fact it was very important for the analysis of [22] that the black holes they studied had negative specific heat. The charged black holes at the center of the hairy solutions here all have positive specific heat.[12]

We also note that the Gubser Mitra instability [23, 24] afflicts three equal charge black holes only when the black holes in question have large enough charge. It follows that the small black holes primarily studied in this paper do not suffer from Gubser Mitra type instabilities.[13]

It is conceivable that the solutions presented in this paper might suffer from further superradiant instabilities, once embedded in IIB theory on $AdS_5 \times S^5$. In order to see why this might be the case, let us recall once again why the field ϕ — dual to the chiral Yang Mills operator $TrX^2 + TrY^2 + TrZ^2$ condensed in the presence of very near extremal charged RNAdS black hole. The reason is simply that the energy $\Delta = 2$ of this field is equal to its charge $e = 2$. As a consequence the Boltzmann suppression factor, $e^{-\beta(\Delta - e)}$ of this mode exceeds unity when $\mu > 1$ causing this mode to Bose condense. However exactly the same reasoning applies to, for instance, the field ϕ_n dual to the chiral operator $TrX^n + TrY^n + TrZ^n$ all of which have $\Delta = e$.[14] It seems likely that there exist other hairy solutions in which some linear combination of ϕ_n (rather than simply ϕ_2) condense.[15] It is important to know whether any solution of this form has higher entropy than the black holes with pure ϕ_2 condensate presented in this paper. If this is the case then the hairy black holes of our paper would likely suffer from superradiant instabilities towards the condensation to the entropically dominant black hole. On the other hand the black holes of this paper, with ϕ_2, the lightest chiral scalar operator that preserves all discrete symmetries of the problem, as the only condensate, are quite special. It seems quite plausible to us that the solution presented in this paper has the largest entropy of all the hairy solutions with

[10] To see this let the sphere be given by equations $|z_1|^2 + |z_2|^2 + |z_3|^2 = 1$ where z_i are the three complex embedding coordinates. A black hole we study is located at $|z_1| = |z_2| = |z_3| = \frac{1}{\sqrt{3}}$, and moves with speed $\frac{(1-\delta)}{\sqrt{3}}$ in each of the three orthogonal planes. Let the proper mass of the black hole be $m_p \propto r_H^7$. Its angular momentum in each plane, $q = r \times p$, is given by $\frac{1}{\sqrt{3}} \times \frac{m_p \gamma (1-\delta)}{\sqrt{3}} = \frac{m_p \gamma (1-\delta)}{3}$ where $\gamma = \frac{1}{\sqrt{1-(1-\delta)^2}}$. The energy of the black hole is $m_p \gamma$.

[11] Were we interested in black holes with small q and $m - 3q \sim \mathcal{O}(q)$ then we would have found $\delta \sim 1$ and $r_H^7 \sim q$. The entropy of the localized black hole would then have been $\propto q^{\frac{8}{7}} > q^{\frac{3}{2}}$. As such black holes can increase their entropy by condensing, they presumably do suffer from Gregory Laflamme type instabilities.

[12] We thank V. Hubeny and M. Rangamani for discussions on this point.

[13] We thank M. Rangamani for a discussion on this point.

[14] This statement is true more generally of every operator in the $\mathcal{N} = 1$ chiral ring of the theory.

[15] In the BPS limit any linear combination of $\rho_n s$ can condense and we have an infinite dimensional moduli space of solutions (see [17, 25]). We expect the introduction of a black hole to lift this moduli space, to a discrete set of solutions.

JHEP11(2011)035

ρ_n condensates. If this is indeed the case then the hairy black hole solutions presented in this paper constitute the thermodynamically dominant saddle point of $\mathcal{N}=4$ Yang Mills very near to supersymmetry; and the entropy of $\mathcal{N}=4$ Yang Mills very near to the BPS bound is given the formula (6.17) below.

To end this introduction we would like to emphasize that the black hole solutions of this paper give a qualitatively different picture of the density of states of $\mathcal{N}=4$ Yang Mills theory at finite charge compared to a picture suggested by RNAdS black holes. As we have seen above, there exist no RNAdS black holes with masses between $m_{BPS}(q)$ and $m_{ext}(q)$, a fact had previously been taken to suggest that, for some mysterious reason, there are less than $\mathcal{O}(N^2)$ states in Yang Mills theory between $m_{BPS}(q)$ and $m_{ext}(q)$. The new black hole solutions of this paper establish, on the other hand, that $\mathcal{N}=4$ Yang Mills theory has $\mathcal{O}(N^2)$ states all the way down to the BPS bound at least at small charge, and plausibly at all values of the charge (see figure 2).[16] The saddle point that governs near BPS behaviour is a mix of a charged Bose condensate and a normal charged fluid. It would be fascinating to find some (even qualitative) confirmation of this picture from a direct field theory analysis.

2 A consistent truncation and its equations of motion

2.1 A consistent truncation of gauged supergravity

$\mathcal{N}=8$ gauged supergravity constitutes a consistent truncation of IIB theory on $AdS_5\times S^5$. In addition to the metric, the bosonic spectrum of this theory consists of 42 scalar fields, 15 gauge fields and 12 two form fields. The scalars transform in the $\mathbf{20}+\mathbf{10_c}+\mathbf{1}+\mathbf{1}$ of SO(6), the gauge fields transform in the 15 dimensional adjoint representation, while the two form fields transform in the $\mathbf{6}_c$ representation of SO(6).

It has been shown [26] that $\mathcal{N}=8$ gauged supergravity admits a further consistent truncation that retains only the scalars in the **20** and the vector fields in the **15** together with the metric, setting all other fields to zero. The action for this consistent truncation is given by [26]

$$\begin{aligned} S=\frac{1}{16\pi G_5}\int\sqrt{g}\Big[R-\frac{1}{4}T^{-1}_{ij}\left(D_\mu T_{jk}\right)T^{-1}_{kl}\left(D^\mu T_{li}\right)-\frac{1}{8}T^{-1}_{ik}T^{-1}_{jl}F^{ij}_{\mu\nu}(F^{kl})^{\mu\nu}-V \\ -\frac{1}{48}\epsilon_{i_1\cdots i_6}\left(F^{i_1i_2}F^{i_3i_4}A^{i_5i_6}-F^{i_1i_2}A^{i_3i_4}A^{i_5j}A^{ji_6}+\frac{2}{5}A^{i_1i_2}A^{i_3j}A^{ji_4}A^{i_5k}A^{ki_6}\right)\Big] \end{aligned} \tag{2.1}$$

where

$$\begin{aligned} V&=\frac{1}{2}\left(2T_{ij}T_{ij}-(T_{ii})^2\right)\\ F^{ij}&=dA^{ij}+A^{ik}\wedge A^{kj}\\ D_\mu T_{ij}&=\partial_\mu T_{ij}+A^{ik}_\mu T_{kj}+A^{jk}_\mu T_{ik}\\ G_5&=\frac{\pi}{2N^2} \end{aligned} \tag{2.2}$$

[16] This difference is starkest in the limit of large charge, i.e. in the Poincare Patch limit. The energy density, ρ_E, of RNAdS black branes is bounded from below by $c\rho_Q^{\frac{4}{3}}$ where ρ_Q is the charge density. Figure 2, on the other hand predicts that the energy density of a charged black brane can be arbitrarily small at any given value of the charge density.

JHEP11(2011)035

Here $(i, j, \cdots)$ denote the SO(6) vector indices and $(\mu, \nu, \cdots)$ are the space time indices. T_{ij} are symmetric unimodular (i.e. T_{ij} is a matrix of unit determinant) SO(6) tensors. Further N is the rank of the gauge group of the dual $\mathcal{N} = 4$ Yang Mills theory, and we work in units in which the AdS_5 with unit radius solves (2.1).

We will now describe a further consistent truncation of (2.1). For this purpose we find it useful to move to a complex basis for the SO(6) vector indices that appear summed in (2.1). Let $(x_j \quad j = 1, \cdots, 6)$ denote SO(6) Cartesian directions. We define the complex coordinates

$$x_{2j-1} + i x_{2j} = z_j, \quad x_{2j-1} - i x_{2j} = \bar{z}_j \quad j = 1, \cdots, 3$$

We will now argue that the restriction

$$\begin{aligned} T_{z_1 z_1} &= T_{z_2 z_2} = T_{z_3 z_3} = \frac{\phi}{4} \\ T_{\bar{z}_1 \bar{z}_1} &= T_{\bar{z}_2 \bar{z}_2} = T_{\bar{z}_3 \bar{z}_3} = \frac{\phi^*}{4} \\ T_{z_1 \bar{z}_1} &= T_{z_2 \bar{z}_2} = T_{z_3 \bar{z}_3} = \frac{\sqrt{4 + \phi\phi^*}}{4} \\ A_\mu^{z_1 \bar{z}_1} &= A_\mu^{z_2 \bar{z}_2} = A_\mu^{z_3 \bar{z}_3} = \frac{A_\mu}{2i} \\ \text{All} \quad &\text{Others} = 0 \end{aligned} \tag{2.3}$$

constitutes a consistent truncation of (2.1). To see this is the case note that the permutations of labels $(1, 2, 3)$, as also separate rotations by π in the z_1, z_2 and z_3 planes, can each be generated by separate SO(6) gauge transformations. It follows that these discrete transformations are symmetries of (2.1). Now it is easy to convince oneself that (2.3) is the most general field configuration of (2.1) that is invariant separately under each of these four discrete symmetries. It follows that (2.3) is a consistent truncation of the system (2.1).

The consistent truncation (2.3) is governed by the Lagrangian

$$\begin{aligned} S &= \frac{1}{8\pi G_5} \int \sqrt{g} \Big[\frac{1}{2}(R + 12) - \frac{3}{8} F_{\mu\nu} F^{\mu\nu} - \frac{3}{16} \left(|D_\mu \phi|^2 - \frac{\partial_\mu(\phi\phi^*)\partial^\mu(\phi\phi^*)}{4(4 + \phi\phi^*)} - 4\phi\phi^* \right) \\ &\qquad + \frac{1}{8\sqrt{g}} \epsilon^{\alpha\beta\gamma\mu\nu} F_{\alpha\beta} F_{\gamma\mu} A_\nu \Big] \\ &= \frac{N^2}{4\pi^2} \int \sqrt{g} \Big[\frac{1}{2}(R + 12) - \frac{3}{8} F_{\mu\nu} F^{\mu\nu} - \frac{3}{16} \left(|D_\mu \phi|^2 - \frac{\partial_\mu(\phi\phi^*)\partial^\mu(\phi\phi^*)}{4(4 + \phi\phi^*)} - 4\phi\phi^* \right) \\ &\qquad + \frac{1}{8\sqrt{g}} \epsilon^{\alpha\beta\gamma\mu\nu} F_{\alpha\beta} F_{\gamma\mu} A_\nu \Big] \\ D_\mu \phi &= \partial_\mu \phi - 2i A_\mu \phi \\ F_{\mu\nu} &= \partial_\mu A_\nu - \partial_\nu A_\mu \end{aligned} \tag{2.4}$$

JHEP11(2011)035

Note that ϕ has charge 2 and $m^2 = -4$. Under the AdS/CFT dictionary this field maps to an operator of dimension $\Delta = 2$. Note also that the kinetic term of the gauge field has the factor prefactor $\frac{3}{8}$ rather than the (more usual) $\frac{1}{4}$ as employed, for instance, in [14].[17]

2.2 Equations of motion

We now list the equations of motion that follow from varying (2.4). We find the Einstein equation

$$R_{\mu\nu} - \frac{1}{2}g_{\mu\nu}R - 6g_{\mu\nu} = -\frac{3}{2}T^{EM}_{\mu\nu} + \frac{3}{8}T^{mat}_{\mu\nu} \tag{2.5}$$

where

$$\begin{aligned} T^{EM}_{\mu\nu} =& F_\mu{}^\sigma F_{\sigma\nu} - \frac{1}{4}g_{\mu\nu}F^{\alpha\sigma}F_{\sigma\alpha} \\ T^{mat}_{\mu\nu} =& \frac{1}{2}\left[D_\mu\phi\,(D_\nu\phi)^* + D_\nu\phi\,(D_\mu\phi)^*\right] - \frac{1}{2}g_{\mu\nu}|D_\sigma\phi|^2 + 2\phi\phi^* g_{\mu\nu} \\ & - \frac{1}{4(4+\phi\phi^*)}\left[\partial_\mu(\phi\phi^*)\partial_\nu(\phi\phi^*) - \frac{1}{2}g_{\mu\nu}[\partial_\sigma(\phi\phi^*)]^2\right] \end{aligned} \tag{2.6}$$

the Maxwell equation

$$\nabla_\sigma F_\mu{}^\sigma = \frac{i}{4}\left[\phi(D_\mu\phi)^* - \phi^* D_\mu\phi\right] + \frac{1}{4\sqrt{g}}g_{\mu\sigma}\epsilon^{\sigma\alpha\beta\gamma\nu}F_{\alpha\beta}F_{\gamma\nu} \tag{2.7}$$

and the scalar equation

$$D_\mu D^\mu\phi + \phi\left[\frac{[\partial_\sigma(\phi\phi^*)]^2}{4(4+\phi\phi^*)^2} - \frac{\nabla^2(\phi\phi^*)}{2(4+\phi\phi^*)} + 4\right] = 0. \tag{2.8}$$

In this paper we study static spherically symmetric configurations of the system (2.4) We adopt a Schwarzschild like gauge and set

$$\begin{aligned} ds^2 &= -f(r)dt^2 + g(r)dr^2 + r^2 d\Omega_3^2 \\ A_t &= A(r) \\ A_r &= A_i = 0 \\ \phi &= \phi^* = \phi(r) \end{aligned} \tag{2.9}$$

The four unknown functions $f(r)$, $g(r)$, $A(r)$ and $\phi(r)$ are constrained by Einstein's equations, the Maxwell equations and the scalar equations. It is possible to demonstrate

[17] Consequently gauge fields and chemical potentials in this paper and [14] are related by

$$A_{here} = \sqrt{\frac{2}{3}}A_{there}, \quad \mu_{here} = \sqrt{\frac{2}{3}}\mu_{there}$$

Note also that G_5 was set to to unity in [14], while $G_5 = \frac{\pi}{2N^2}$ in this paper. It follows that

$$\frac{M_{here}}{N^2} = \frac{2}{\pi}M_{there}, \quad \frac{S_{here}}{N^2} = \frac{2}{\pi}S_{there}, \quad \frac{Q_{here}}{N^2} = \frac{2}{\pi}\sqrt{\frac{1}{6}}Q_{there}$$

The factor of $\sqrt{\frac{1}{6}}$ above ensures that $TdS_{there} = dM_{there} - \mu_{there}dQ_{there}$ implies $TdS_{here} = dM_{here} - 3\mu_{here}dQ_{here}$ as is required on on physical grounds.

JHEP11(2011)035

that f, g, A, ϕ are solutions to the equations of motion if and only if

$$\begin{aligned}
E_1 &= g(r)\left(-\frac{3\left[A(r)^2+f(r)\right]\phi(r)^2}{4f(r)}-\frac{3}{r^2}-6\right)\\
&\quad+\frac{3}{4}\left[-\frac{\phi'(r)^2}{\phi(r)^2+4}+\frac{A'(r)^2+\frac{2f'(r)}{r}}{f(r)}+\frac{4}{r^2}\right]=0\\
E_2 &= \frac{g(r)^2}{f(r)}\left(-A(r)^2\phi(r)^2-\frac{A'(r)^2}{g(r)}\right)+\left(\frac{2rg'(r)-4g(r)}{r^2}\right)\\
&\quad-\frac{g(r)\phi'(r)^2}{\phi(r)^2+4}+\left(\frac{4}{r^2}+8+\phi(r)^2\right)g(r)^2=0\\
E_3 &= 2A(r)g(r)\phi(r)^2+A'(r)\left(\frac{f'(r)}{f(r)}+\frac{g'(r)}{g(r)}-\frac{6}{r}\right)-2A''(r)=0\\
E_4 &= \left(\frac{1}{4+\phi(r)^2}\right)\nabla^2\phi(r)+\left(1+\frac{A(r)^2}{f(r)}-\frac{\phi'(r)^2}{g(r)\left[\phi(r)^2+4\right]^2}\right)\phi(r)=0
\end{aligned} \tag{2.10}$$

where

$$\nabla^2\phi(r)=\frac{g(r)\left[\left(\frac{f'(r)}{f(r)}+\frac{6}{r}\right)\phi'(r)+2\phi''(r)\right]-g'(r)\phi'(r)}{2g(r)^2}$$

The equations E_1 and E_2 are derived from the rr and tt components of the Einstein equations, E_3 is the t component of the Maxwell equation and E_4 is the equation of the scalar field.

As in [14] the equations (2.10) contain only first derivatives of f and g, but depend on derivatives up to the second order for ϕ and A. It follows that (2.10) admit a 6 parameter set of solutions. One of these solutions is empty AdS_5 space, given by $f(r)=r^2+1$, $g(r)=\frac{1}{1+r^2}$, $A(r)=\phi(r)=0$. We are interested in those solutions to (2.10) that asymptote to AdS space time, i.e. solutions whose large r behaviour is given by

$$\begin{aligned}
f(r) &= r^2+1+\mathcal{O}(1/r^2)\\
g(r) &= \frac{1}{1+r^2}+\mathcal{O}(1/r^6)\\
A(r) &= \mathcal{O}(1)+\mathcal{O}(1/r^2)\\
\phi(r) &= \mathcal{O}(1/r^2)
\end{aligned} \tag{2.11}$$

As in [14] it turns out that these conditions effectively impose two conditions on the solutions of (2.10), so that the system of equations admits a four parameter set of asymptotically AdS solutions. We usually also be interested only in solutions that are regular (in a suitable sense) in the interior. This requirement will usually cut down solution space to distinct classes of two parameter space of solutions; the parameters may be thought of as the mass and charge of the solutions.

JHEP11(2011)035

2.3 RNAdS black holes

The AdS-Reissner-Nordstrom black holes constitute a very well known two parameter set of solutions to the equations (2.10). These solutions are given by

$$\begin{aligned} f(r) &= \frac{\mu^2 R^4}{r^4} - \frac{\left(R^2+\mu^2+1\right)R^2}{r^2} + r^2 + 1 \\ &= \frac{1}{r^4}\left[r^2 - R^2\right]\left[r^4 + r^2(R^2+1) - \mu^2 R^2\right] \\ g(r) &= \frac{1}{f(r)} \\ A(r) &= \mu\left(1 - \frac{R^2}{r^2}\right) \\ \phi(r) &= 0 \end{aligned} \tag{2.12}$$

where μ is the chemical potential of the RNAdS black hole. The function $V(r)$ in (2.12) vanishes at $r = R$ and consequently this solution has a horizon at $r = R$. In fact, it can be shown that R is the outer event horizon provided

$$\mu^2 \leq (1 + 2R^2). \tag{2.13}$$

As explained in [14] and in the introduction, (2.12) is unstable to superradiant decay provided in the presence of field of charge e and minimum energy Δ provided $e\mu > \Delta$. Now our field ϕ has $\Delta = 2$ and $e = 2$. Moreover, in the limit $R \to 0$, RNAdS black holes have $\mu \leq 1$ (this inequality is saturated at extremality). It follows that small extremal black holes lie at the edge of instability, as mentioned in the introduction. We show below that very near extremal RNAdS black holes do in fact suffer from super radiant instabilities.

3 The supersymmetric soliton in perturbation theory

In this section we will construct the analogue of the ground state soliton in [14]. The new feature in here is that the soliton turns out to be supersymmetric (this is obvious at linearized order).

In this section we generate the solitonic solution in perturbation theory. We use only the equations of motion without imposing the constraints of supersymmetry, but check that our final solution is supersymmetric (by verifying the BPS bound order by order in perturbation theory). This method has the advantage that it generalizes in a straightforward manner to the construction of non supersymmetric hairy black holes in subsequent sections.

In section 5 we will revisit this solitonic solution; we will rederive it by imposing the constraints of supersymmetry from the start. That method has the advantage that it permits a relatively simple extrapolation of supersymmetric solutions to large charge.

JHEP11(2011)035

3.1 Setting up the perturbative expansion

We now turn to the description of our perturbative construction. To initiate the perturbative construction of the supersymmetric soliton we set

$$\begin{aligned} f(r) &= 1 + r^2 + \sum_n \epsilon^{2n} f_{2n}(r) \\ g(r) &= \frac{1}{1+r^2} + \sum_{n=1}^{\infty} \epsilon^{2n} g_{2n}(r) \\ A(r) &= 1 + \sum_{n=1}^{\infty} \epsilon^{2n} A_{2n}(r) \\ \phi(r) &= \frac{\epsilon}{1+r^2} + \sum_{n=1}^{\infty} \phi_{2n+1}(r)\epsilon^{2n+1} \end{aligned} \tag{3.1}$$

and plug these expansions into (2.10). We then expand out and solve these equations order by order in ϵ. All equations are automatically solved up to $\mathcal{O}(\epsilon)$. At order ϵ^{2n} the last equation in (2.10) is trivial while the first three take the form

$$\begin{aligned} \frac{d}{dr}\left(r^2(1+r^2)^2 g_{2n}(r)\right) &= P^{(g)}_{2n}(r) \\ \frac{d}{dr}\left(\frac{f_{2n}(r)}{1+r^2}\right) &= \frac{2(1+2r^2)}{r} g_{2n}(r) + P^{(f)}_{2n}(r) \\ \frac{d}{dr}\left(r^3 \frac{dA_{2n}(r)}{dr}\right) &= P^{(A)}_{2n}(r). \end{aligned} \tag{3.2}$$

On the other hand, at order ϵ^{2n+1} the first three equations in (2.10) is trivial while the last equation reduces to

$$\frac{d}{dr}\left(\frac{r^3}{1+r^2}\frac{d}{dr}\left[(1+r^2)\phi_{2n+1}(r)\right]\right) = P^{(\phi)}_{2n+1}(r) \tag{3.3}$$

Here the source terms $P^{(g)}_{2n}(r)$, $P^{(f)}_{2n}(r)$, $P^{(A)}_{2n}(r)$ and $P^{(\phi)}_{2n+1}(r)$ are completely determined by the solution to lower orders in perturbation theory, and so should be thought of as known functions, in terms of which we wish to determine the unknowns f_{2n}, g_{2n}, A_{2n} and ϕ_{2n+1}.

The equations (3.2) are all easily integrated. It also turns out that all the integration constants in these equations are uniquely determined by the requirements of regularity, normalisability and our definition of ϵ, exactly as in [14]. The solution is given by

$$\begin{aligned} g_{2n}(r) =& \frac{1}{r^2(1+r^2)^2}\left[\int_0^r P^{(g)}_{2n}(s)ds\right] \\ f_{2n}(r) =& -(1+r^2)\int_r^{\infty}\left[\frac{2(1+2s^2)}{s} g_{2n}(s) + P^{(f)}_{2n}(s)\right] ds \\ A_{2n}(r) =& -\int_r^{\infty}\frac{ds}{s^3}\left(\int_0^s P^{(A)}_{2n}(s')ds'\right) \\ \phi_{2n+1}(r) =& -\frac{1}{1+r^2}\left[\int_r^{\infty} ds\left(\frac{1+s^2}{s^3}\right)\left(\int_0^s P^{(\phi)}_{2n+1}(s')ds'\right)\right] \end{aligned} \tag{3.4}$$

JHEP11(2011)035

3.2 The soliton up to $\mathcal{O}(\epsilon^9)$

The perturbative procedure outlined in this subsection is very easily implemented to arbitrary order in perturbation theory. In fact, by automating the procedure described above, we have implemented this perturbative series to 17th order in a Mathematica programme. In the rest of this subsection we content ourselves with a presentation of our results to $\mathcal{O}(\epsilon^9)$.

$$\begin{aligned} g_2(r) &= 0 \\ f_2(r) &= -\frac{1}{4(1+r^2)} \\ A_2(r) &= -\frac{1}{8(1+r^2)} \\ \phi_3(r) &= \frac{1}{8(1+r^2)^3} \end{aligned} \tag{3.5}$$

$$\begin{aligned} g_4(r) &= \frac{r^4}{192(1+r^2)^5} \\ f_4(r) &= -\frac{r^4}{192(1+r^2)^3} \\ A_4(r) &= -\frac{r^4+3r^2+3}{384\left(r^2+1\right)^3} \\ \phi_5(r) &= \frac{6r^4+4r^2+55}{2304\left(r^2+1\right)^5} \end{aligned} \tag{3.6}$$

$$\begin{aligned} g_6(r) &= \frac{r^4\left(4r^4+15r^2+20\right)}{7680\left(r^2+1\right)^7} \\ f_6(r) &= -\frac{12r^8+45r^6+60r^4+20r^2+5}{23040\left(r^2+1\right)^5} \\ A_6(r) &= -\frac{6r^8+30r^6+60r^4+55r^2+25}{23040\left(r^2+1\right)^5} \\ \phi_7(r) &= \frac{120r^8+460r^6+1095r^4+558r^2+2368}{460800\left(r^2+1\right)^7} \end{aligned} \tag{3.7}$$

$$\begin{aligned} g_8(r) &= \frac{r^4\left(169r^8+1024r^6+2640r^4+3320r^2+2180\right)}{2211840\left(r^2+1\right)^9} \\ f_8(r) &= -\frac{\left(5\left(169r^8+1024r^6+2580r^4+3344r^2+2288\right)r^2+3096\right)r^2+516}{11059200\left(r^2+1\right)^7} \\ A_8(r) &= -\frac{\left(5\left(\left(169\left(r^4+7r^2+21\right)r^2+5819\right)r^2+5543\right)r^2+14721\right)r^2+4191}{22118400\left(r^2+1\right)^7} \\ \phi_9(r) &= \frac{\left(5\left(1014r^8+6124r^6+18257r^4+30484r^2+36676\right)r^2+75784\right)r^2+155759}{132710400\left(r^2+1\right)^9} \end{aligned} \tag{3.8}$$

The soliton obeys the BPS relation $m = 3q$ to the order to which we have carried out our computation (we present more details of the thermodynamics in section 6).

JHEP11(2011)035

4 The hairy black hole in perturbation theory

4.1 Basic perturbative strategy

We will now present our perturbative construction of hairy black hole solutions. In order to set up the perturbative expansion we expand the metric gauge field and the scalar fields as

$$\begin{aligned} f(r) &= \sum_{n=0}^{\infty} \epsilon^{2n} f_{2n}(r) \\ g(r) &= \sum_{n=0}^{\infty} \epsilon^{2n} g_{2n}(r) \\ A(r) &= \sum_{n=0}^{\infty} \epsilon^{2n} A_{2n}(r) \\ \phi(r) &= \sum_{n=0}^{\infty} \epsilon^{2n+1} \phi_{2n+1}(r) \end{aligned} \tag{4.1}$$

where the unperturbed solution is taken to be the RNAdS black hole

$$\begin{aligned} f_0(r,R) = V(r), \quad g_0(r,R) &= \frac{1}{V(r)} \\ A_0(r,R) &= \mu_0 \left(1 - \frac{R^2}{r^2}\right) \\ V(r) &= 1 + r^2 \left(1 - \frac{R^2\mu_0^2 + R^2 + R^4}{r^4} + \frac{R^4\mu_0^2}{r^6}\right) \end{aligned} \tag{4.2}$$

The chemical potential of our final solution will be given by an expression of the form

$$\begin{aligned} \mu = \mu(\epsilon, R) &= \sum_{n=0} \epsilon^{2n} \mu_{2n}(R) \\ \mu_{2n}(R) &= \sum_{k=0}^{\infty} \mu_{(2n,2k)} R^{2k} \\ \mu_{(0,0)} &= 1 \end{aligned} \tag{4.3}$$

Note that, at the leading order in the perturbative expansion, $\mu = 1$.

Our basic strategy is to plug the expansion (4.1) into the equations of motion and then to recursively solve the later in a power series in ϵ. We expand our equations in a power series in ϵ. At each order in ϵ we have a set of linear differential equations (see below for the explicit form of the equations), which we solve subject to the requirements of the normalisability of $\phi(r)$ and $f(r)$ at infinity together with the regularity of $\phi(r)$ and the metric at the horizon. These four physical requirements turn out to automatically imply that $A(r = R) = 0$ i.e. the gauge field vanishes at the horizon, as we would expect of a stationary solution. These four physical requirements determine 4 of the six integration constants in the differential equation, yielding a two parameter set of solutions. We fix the remaining two integration constants by adopting the following conventions to label our solutions: we require that $\phi(r)$ fall off at infinity like $\frac{\epsilon}{r^2}$ (definition of ϵ) and that

JHEP11(2011)035

the horizon area of our solution is $2\pi^2 R^3$ (definition of R). This procedure completely determines our solution as a function of R and ϵ. We can then read of the value of μ in (4.3) on our solution from the value of the gauge field at infinity.

As in [14], the linear differential equations that arise in perturbation theory are difficult to solve exactly, but are easily solved in a power series expansion in R, by matching near field, intermediate field and far field solutions. At every order in ϵ we thus have a solution as an expansion in R. Our final solutions are, then presented in a double power series expansion in ϵ and R.

4.2 Perturbation theory at $\mathcal{O}(\epsilon)$

In this section we present a detailed description of the implementation of our perturbative expansion at $\mathcal{O}(\epsilon)$. The procedure described in this subsection applies, with minor modifications, to the perturbative construction at $\mathcal{O}(\epsilon^{2m+1})$ for all m.

Of course all equations are automatically obeyed at $\mathcal{O}(\epsilon^0)$. The only nontrivial equation at $\mathcal{O}(\epsilon)$ is $D^2\phi + 4\phi = 0$ where $D_\mu = \nabla_\mu - 2iA_\mu$ is the linearized gauge covariantised derivative about the background (4.2). We will now solve this equation subject to the constraints of normalisability at infinity, regularity at the horizon, and the requirement that

$$\phi(r) \sim \frac{\epsilon}{r^2} + \mathcal{O}(1/r^4)$$

at large r.

4.2.1 Far field region ($r \gg R$)

Let us first focus on the region $r \gg R$. In this region the black hole (4.2)

$$\begin{aligned} f_0(r) &= \frac{\mu_0^2 R^4}{r^4} - \frac{\left(R^2+\mu^2+1\right)R^2}{r^2} + r^2 + 1 \\ &= \frac{1}{r^4}\left[r^2 - R^2\right]\left[r^4 + r^2(R^2+1) - \mu_0^2 R^2\right] \\ g_0(r) &= \frac{1}{f(r)} \\ A_0(r) &= \mu_0\left(1 - \frac{R^2}{r^2}\right) \\ \mu_0 &= \sum_{k=0}^{\infty} R^{2k}\mu_{(0,2k)} \\ \mu_{(0,0)} &= 1 \end{aligned} \tag{4.4}$$

is a small perturbation about global AdS space. For this reason we expand

$$\phi_1^{\text{out}}(r) = \sum_{k=0}^{\infty} R^{2k}\phi_{(1,2k)}^{\text{out}}(r), \tag{4.5}$$

where the superscript *out* emphasises that this expansion is good at large r. In the limit $R \to 0$, (4.4) reduces to global AdS space time with $A_t = 1$. A stationary linearised

JHEP11(2011)035

fluctuation about this background is gauge equivalent to a linearised fluctuation with time dependence e^{-it} about global AdS space with $A_t = 0$ (A_t is the temporal component of the gauge field). The required solution is simply the ground state excitation of an $m^2 = -4$ minimally coupled scalar field about global AdS and is given by

$$\phi^{\rm out}_{(1,0)}(r) = \frac{1}{1+r^2} \tag{4.6}$$

The overall normalisation of the mode is set by our definition of ϵ which implies

$$\phi^{\rm out}_{(1,0)}(r) = \frac{1}{r^2} + \mathcal{O}(1/r^4).$$

We now plug (4.5) into the equations of motion $D^2\phi = 0$ and expand to $\mathcal{O}(R^2)$ to solve for $\phi^{\rm out}_{(1,2)}$. Here D^2 is the gauge covariant Laplacian about the background (4.4). Now

$$(D^2)^{\rm out} = (D_0^2)^{\rm out} + R^2 (D_2^2)^{\rm out} + \dots$$

where $(D_0^2)^{\rm out}$ is the gauge covariant Laplacian about global AdS space time with background gauge field $A_t = 1$. It follows that, at $\mathcal{O}(R^2)$,

$$(D_0^2)^{\rm out}\phi^{\rm out}_{(1,2)} = -(D_2^2)^{\rm out}\phi^{\rm out}_{(1,0)} = -(D_2^2)^{\rm out}\left[\frac{1}{1+r^2}\right]$$

This equation is easily integrated and we find

$$\phi^{\rm out}_{(1,2)}(r) = -\left(\frac{1}{1+r^2}\right)\left(\frac{\mu_{(0,2)}}{r^2} - 2\left[\mu_{(0,2)}-2\right]\log(r) + \left[\mu_{(0,2)}-2\right]\log\left(r^2+1\right) + \frac{2}{r^2+1}\right) \tag{4.7}$$

We could iterate this process to generate $\phi^{\rm out}_{(1,2k)}$ upto any desired order k. The equations we need to solve, at order $\mathcal{O}(R^{2k})$, takes the form

$$\frac{d}{dr}\left(\frac{r^3}{1+r^2}\frac{d}{dr}\left[(1+r^2)\phi^{\rm out}_{(1,2k)}(r)\right]\right) = P^{\rm out}_{(1,2k)}(r) \tag{4.8}$$

where $P^{\rm out}_{(1,2k)}(r)$ is a source function, whose form is determined by the results of the expansion at lower orders in perturbation theory.

As in (4.7), it turns out that the expressions $\phi^{\rm out}_{(1,2k)}$ are increasingly singular as $r \to 0$. In fact it may be shown that the most singular piece of $\phi^{\rm out}_{(1,2k)}$ scales like $\frac{1}{r^{2k}}$, upto logarithmic corrections. In other words the expansion of $\phi^{\rm out}$ in powers of R^2 is really an expansion in $\frac{R^2}{r^2}$ (upto log corrections) and breaks down at $r \sim R$.

To end this subsection we summarize our results to $\mathcal{O}(R^2)$. We have

$$\begin{aligned}\phi_1^{\rm out} = &\frac{1}{1+r^2}\\ &+ R^2\left[-\left(\frac{1}{1+r^2}\right)\left(\frac{\mu_{(0,2)}}{r^2} - 2\left[\mu_{(0,2)}-2\right]\log(r) + \left[\mu_{(0,2)}-2\right]\log\left(r^2+1\right) + \frac{2}{r^2+1}\right)\right]\\ &+ \mathcal{O}\left(\frac{R^4}{r^4}\right)\end{aligned} \tag{4.9}$$

JHEP11(2011)035

Expanding $\phi_1^{\rm out}(r)$ in a Taylor series about $r=0$ we find

$$\begin{aligned}\phi_1^{\rm out}(r) = & \left[1 - r^2 + \mathcal{O}(r^4)\right] \\ & + R^2\left[\frac{\mu_{(0,2)}}{r^2} + (\mu_{(0,2)} - 2)(2\log(r) + 1) + \mathcal{O}(r^2)\right] \\ & + \mathcal{O}\left(\frac{R^4}{r^4}\right)(1 + \mathcal{O}(r^2)) + \dots\end{aligned} \tag{4.10}$$

Note that this result depends on the as yet unknown parameter $\mu_{(0,2)}$. This quantity will be determined below by matching with the intermediate field solution of the next subsection.

4.2.2 Intermediate field region $r \ll 1$ and $(r - R) \gg R^3$

Let us now turn to intermediate region $R^3 \ll r - R \ll 1$. Over these length scales the small black hole is far from a small perturbation about AdS_5 space. Instead the simplification in this region stems first from the fact that we focus on radial distances of order R ($r \sim R \ll 1$). Over these small length scales the background gauge field, which is of order unity, is negligible compared to the mass scale set by the horizon radius $\frac{1}{R}$.

A second simplification results from the fact that we insist that $(r - R) \gg R^3$, i.e. we do not let our length scales become too small. At these distances the back hole that we perturb around are effectively extremal (rather than slightly non extremal) at leading order. Moreover the black hole may also be thought of (at leading order) as a small black hole in flat rather than global AdS space.[18]

In this region it is convenient to work in a rescaled radial coordinate $y = \frac{r}{R}$ and a rescaled time coordinate $\tau = \frac{t}{R}$. Note that the near field region consists of space time points with y of order unity (but not too near to unity). Points with y of order $\frac{1}{R}$ (or larger) and $y - 1$ of order $\mathcal{O}(R^2)$ (or smaller) are excluded from the considerations of this subsection.

The metric and the gauge field of the background black hole take the form

$$\begin{aligned} ds^2 =& R^2\left[-V(y)d\tau^2 + \frac{dy^2}{V(y)} + y^2 d\Omega_3^2\right] \\ V(y) =& \left[1 - \frac{1}{y^2}\right]\left[1 - \frac{\mu_0^2}{y^2} + R^2(1 + y^2)\right] \\ A_\tau(y) =& R\mu_0\left(1 - \frac{1}{y^2}\right) \\ \mu_0 =& \sum_{k=0}^{\infty} R^{2k}\mu_{(0,2k)} \\ \mu_{(0,0)} =& 1 \end{aligned} \tag{4.11}$$

[18] As we will see below, deviations of the black hole from extremality (and deviations of the form of its metric from the metric of a flat space black hole) are crucial to dynamics at $r - R \sim R^3$, but are small perturbations on dynamics when $(r - R) \gg R^3$.

JHEP11(2011)035

As in the previous subsection we expand

$$\phi_1^{\rm mid}(y) = \sum_{k=0}^{\infty} R^{2k} \phi_{(1,2k)}^{\rm mid}(y) \tag{4.12}$$

To determine the unknown functions in this expansion, we must solve the equation $D^2\phi^{\rm mid} = 0$, where D^2 is the gauge covariant Laplacian about the background (4.11). Our solutions must match with the far field expansion of the previous subsection, and the near field expansion of the next subsection, but are subject to no intrinsic boundary regularity requirements.

At $\mathcal{O}(R^{2k})$ our equations take the form

$$\frac{1}{y^3}\frac{d}{dy}\left(y^3 V_0(y)\frac{d}{dy}\right)\phi_{(1,2k)}^{\rm mid}(y) = P_{(1,2k)}^{\rm mid}(y) \tag{4.13}$$

where

$$V_0(y) = \left(1 - \frac{1}{y^2}\right)^2$$

and $P_{(1,2k)}^{\rm mid}(y)$ is a source term determined (recursively) by the perturbative procedure. Ignoring the requirements of matching, for a moment, the solution to this equation is determined only upto two integration constants at every order. It turns out that $\phi_{(1,2k)}^{\rm mid}(y)$ grows like y^{2k} (upto possible logarithmic corrections) at large y and grows like $\frac{1}{(y-1)^k}$ as y approaches unity. It follows that the expansion (4.13) is good only when

$$R^2 \ll (y-1) \ll \frac{1}{R}$$

We now work out the explicit solutions at low orders. $P_{(1,0)}^{\rm mid}(y) = 0$ vanishes, so the solution for $\phi_{(1,0)}^{\rm mid}(y)$ is particularly simple, and takes the form

$$\phi_{(1,0)}^{\rm mid}(y) = c_1 + \frac{c_2}{y^2-1}$$

c_1 and c_2 are the two constants. It is easy to check that the matching of $\phi_{(1,0)}^{\rm mid}(y)$ with $\phi_{(1,0)}^{\rm out}(r)$ sets $c_1 = 1$. It follows on general grounds that matching with the (as yet undetermined) near field solution forces c_2 to vanish. This is because, were c_2 to be nonzero, it would match onto a near field solution of order $\mathcal{O}\left(\frac{1}{R^2}\right)$ in the near field region (see the next subsection for details), violating the requirement that that our solution has a smooth $R \to 0$ limit.

We can now iterate the procedure of this subsection to solve to order in R^2 in the intermediate field region. We find

$$\begin{aligned}
\phi_{(1,0)}^{\rm mid}(y) =& 1 \\
\phi_{(1,2)}^{\rm mid}(y) =& -y^2 - 2\log(y^2-1) + c_3 + \frac{c_4}{y^2-1}
\end{aligned} \tag{4.14}$$

so that

Here c_3 and c_4 are the two integration constants. c_3 may immediately be determined by matching with the far field solution; it turns out that this procedure also determines $\mu_{(0,2)} = 0$, the chemical potential that was left undetermined in the previous subsection. In order to perform this matching we expand $\phi_1^{\rm mid}(y)$ about large y

$$\phi_1^{\rm mid}(y) = 1 + R^2 \left[-y^2 + c_3 - 4\log(y) + \mathcal{O}\left(\frac{1}{y^2}\right)\right] + \mathcal{O}(R^4 y^4) \tag{4.15}$$

The strategy is now to substitute $y = \frac{r}{R}$ in (4.15) and then to compare with (4.10). Of course one should only compare those terms that are reliable in both expansions. Terms of order $R^{2m} r^{2n}$ are reliably computed from (4.15) only when $m + n \leq 1$. Terms of the same form are reliably computed from (4.10) only when $m \leq 1$. Consequently, the only terms that one may reliably compare are those of the form $\mathcal{O}(R^0 r^0)$, $\mathcal{O}(R^0 r^2)$, $\mathcal{O}(R^2 r^0)$ together with logarithmic corrections. The difference between the sum of the corresponding terms (in (4.15) and (4.10)) is given by

$$\text{Difference} = R^2 \left(\frac{\mu_{(0,2)}}{r^2} + 2\mu_{(0,2)} \log(r) + \mu_{(0,2)} - 2 - 4\log(R) - c_3 \right)$$

and vanishes provided $\mu_{(0,2)} = 0$ and $c_3 = -2(1 + 2\log R)$ so that

$$\phi_1^{\rm mid}(y) = 1 + R^2 \left(-y^2 - 2\log(y^2 - 1) - 2(1 + 2\log R) + \frac{c_4}{y^2 - 1} \right) + \mathcal{O}(R^4) \tag{4.16}$$

c_4 will be determined below by matching to the near field region. To facilitate this matching in the next subsection, we present the expansion of $\phi_1^{\rm mid}(y)$ expanded around $y = 1$.

$$\begin{aligned} \phi_1^{\rm mid}(y) = 1 + R^2 \left[\frac{c_4}{2(y-1)} - \left(\frac{c_4}{4} + 3 + 2\log 2 + 4\log R \right) - 2\log(y-1) + \mathcal{O}(y-1) \right] \\ + \mathcal{O}\left(\frac{R^4}{(y-1)^2} \right) \end{aligned} \tag{4.17}$$

4.2.3 Near field region $(r - R) \ll R$ or $(y - 1) \ll 1$

In this subsection we will determine the scalar field in the near field region $r - R \ll R$. More particularly, we will work in terms of a further rescaled radial coordinate $z = \frac{y-1}{R^2}$. Note that the black hole horizon occurs at $z = 0$. Note points at finite z are located at $r - R \sim R^3$ or $y - 1 \sim R^2$. It is also convenient to work with the new time coordinate $T = Rt = R^2\tau$ As in the previous subsection, the background gauge field makes a small direct contribution to dynamics in this region. However deviation of the black hole metric from extremality (and the difference between an AdS and flat space black hole metric) are all important in this region, and have to be dealt with exactly rather than perturbatively.

JHEP11(2011)035

In the new coordinates, the metric and gauge field take the form

$$\begin{aligned}
\frac{ds^2}{R^2} =& -V(z)dT^2 + \frac{dz^2}{V(z)} + (1+R^2z)^2 d\Omega_3^2 \\
A_T(y) =& \frac{\mu_0}{R}\left(1 - \frac{1}{(1+R^2z)^2}\right) = 2\mu_0 R z^2 + \mathcal{O}(R^3 z^4) \\
\mu_0 =& \sum_{k=0}^{\infty} R^{2k}\mu_{(0,2k)} \\
\mu_{(0,0)} =& 1, \quad \mu_{(0,2)} = 0 \\
V(z) =& \frac{1}{R^4} \times \left(1 + \frac{\mu_0^2}{(R^2z+1)^4} - \frac{\mu_0^2+1+R^2}{(R^2z+1)^2} + R^2\left(1+R^2z\right)^2\right) \\
=& 4z(1+z) + \mathcal{O}(R^2)
\end{aligned} \tag{4.18}$$

As in previous subsections we expand the field $\phi(z)$ as

$$\phi_1^{\rm in}(z) = \sum_{k=0}^{\infty} R^{2k}\phi_{(1,2k)}^{\rm in}(z) \tag{4.19}$$

and plug this expansion into the equations of motion. At $\mathcal{O}(R^{2k})$ the equations take the form

$$\frac{d}{dz}\left(4z(1+z)\frac{d}{dz}\right)\phi_{(1,2k)}^{\rm in}(z) = P_{(1,2k)}^{\rm in}(z) \tag{4.20}$$

where, as usual, $P_{(1,2k)}^{\rm in}(z)$ is a source term whose form is determined from the results of perturbation theory at lower orders. We solve the equation (4.20) subject to the requirement of regularity at $z=0$. It is possible to argue that the solution to $\phi_{(1,2k)}^{\rm in}(z)$ behaves like z^{k-1} (upto logarithmic corrections) at large z.

At lowest order ($k=0$) $P_{(1,0)}^{\rm in}(y) = 0$ vanishes, and the unique regular solution for $\phi_{(1,0)}^{\rm in}(y)$ is the constant. Matching determines the value of the constant to be unity.

At next order, (i.e. $\mathcal{O}(R^2)$) the solution — after imposing the requirement of regularity — is given by

$$\begin{aligned}
\phi_{(1,2)}^{\rm in}(z) &= 1 \\
\phi_{(1,2)}^{\rm in}(z) &= \alpha - \frac{1}{2}\log^2(z+1) - 2\log(z+1) - {\rm Li}_2(-z)
\end{aligned} \tag{4.21}$$

where α is the constant which we will now determine by matching with the intermediate field solution. Expanding $\phi_1^{\rm in}(z)$ around $z=\infty$ we find

$$\phi^{\rm in}(z) = 1 + R^2\left[\alpha + \frac{\pi^2}{6} - 2\log z + \mathcal{O}\left(\frac{1}{z}\right)\right] \tag{4.22}$$

We now substitute $z = \frac{y-1}{R^2}$ in (4.22) and then compare with (4.17). We find a perfect match provided α and c_4 are chosen to be the following

$$c_4 = 0 \quad \text{and} \quad \alpha = -\left(\frac{\pi^2}{6} + 3 + 2\log 2 + 8\log R\right)$$

JHEP11(2011)035

4.3 Perturbation theory at $\mathcal{O}(\epsilon^2)$

We now briefly outline the procedure used to evaluate the solution at $\mathcal{O}(\epsilon^2)$. We proceed in close imitation to the previous subsection. The main difference is that at this (and all even orders) in the ϵ expansion, perturbation theory serves to determine the corrections to the functions f, g and A rather than the function ϕ. The procedure described here applies, with minor modifications, to the perturbative construction at $\mathcal{O}(\epsilon^{2m})$ for all m.

4.3.1 Far field region, $r \gg R$

When $r \gg R$ we expand

$$\begin{aligned} f_2^{\rm out}(r) &= \sum_{k=0}^{\infty} R^{2k} f^{\rm out}_{(2,2k)}(r) \\ g_2^{\rm out}(r) &= \sum_{k=0}^{\infty} R^{2k} g^{\rm out}_{(2,2k)}(r) \\ A_2^{\rm out}(r) &= \sum_{k=0}^{\infty} R^{2k} A^{\rm out}_{(2,2k)}(r) \end{aligned} \tag{4.23}$$

where

$$\begin{aligned} &f_0^{\rm out}(r) = V(r), \qquad g_0^{\rm out}(r) = \frac{1}{V(r)}, \qquad A_0^{\rm out}(r) = \mu_0 \left(1 - \frac{R^2}{r^2}\right) \\ &\mu_0 = \sum_{k=0}^{\infty} R^{2k} \mu_{(0,2k)} \qquad \mu_{(0,0)} = 1, \qquad \mu_{(0,2)} = 0 \end{aligned} \tag{4.24}$$

As in the previous subsection, we plug this expansion into the equations of motion and solve the resultant equations recursively. The equations take the form

$$\begin{aligned} \frac{d}{dr}\left(r^2(1+r^2)^2 g^{\rm out}_{(2,2k)}(r)\right) &= \text{Source} \\ \frac{d}{dr}\left(\frac{f^{\rm out}_{(2,2k)}(r)}{1+r^2}\right) - \frac{2(1+2r^2)}{r} g^{\rm out}_{(2,2k)}(r) &= \text{Source} \\ \frac{d}{dr}\left(r^3 \frac{dA^{\rm out}_{(2,2k)}(r)}{dr}\right) &= \text{Source}. \end{aligned} \tag{4.25}$$

and may be thought of as the equations governing sourced linearized fluctuations about empty global AdS space with $A_t = 1$.

The equations (4.25) are easily solved by integration. One of the integration constant in the first equation is fixed by the requirement that $f^{\rm out}_{(2,2k)}(r)$ is normalizable (see (2.11)). The remaining three integration constants (one in the first equation and two in the last) will be fixed by matching with the intermediate field solution below.

The constraints of matching are particularly simple at $\mathcal{O}(R^0)$; they require that the solutions for $g^{\rm out}_{(2,0)}$, $f^{\rm out}_{(2,0)}$ and $A^{\rm out}_{(2,0)}$ are all regular at $r = 0$. This is because a far field solution of the form $\frac{1}{r^k}$ would match onto an intermediate solution of the form $\frac{1}{y^k R^k}$. But

JHEP11(2011)035

this contradicts our basic assumption that our solutions have a smooth $R \to 0$ limit. It follows that at $\mathcal{O}(R^0)$[19] all our functions obey the same equations — and boundary conditions — for the 2nd order fluctuations about the supersymmetric soliton and we obtain the same (unique) solution

$$\begin{aligned} g^{\rm out}_{(2,0)}(r) &= 0 \\ f^{\rm out}_{(2,0)}(r) &= -\frac{1}{4(1+r^2)} \\ A^{\rm out}_{(2,0)}(r) &= -\frac{1}{8(1+r^2)} \end{aligned} \tag{4.26}$$

At order $\mathcal{O}(R^2)$ we find

$$\begin{aligned} g^{\rm out}_{(2,2)}(r) &= -\frac{1}{4r^2\,(r^2+1)^3} - \frac{k}{r^2(1+r^2)^2} \\ f^{\rm out}_{(2,2)}(r) &= \frac{3+5r^2}{4r^2(1+r^2)^2} - \frac{1}{1+r^2}\log\left(\frac{1+r^2}{r^2}\right) + \frac{k}{r^2} \\ A^{\rm out}_{(2,2)}(r) &= \frac{1+2r^2}{4r^2(1+r^2)^2} - \frac{1}{2(1+r^2)}\log\left(\frac{1+r^2}{r^2}\right) + \frac{h_1}{4} + \frac{h_2}{4r^2} \end{aligned} \tag{4.27}$$

Here k, h_1 and h_2 are the three undetermined constants, which will be determined by matching with the intermediate field solution. To facilitate this determination below we end this subsection by presenting an expansion of (4.27) about $r = 0$

$$\begin{aligned} g^{\rm out}_2(r) &= R^2\left[-\frac{k+\frac{1}{4}}{r^2} + \mathcal{O}(r^0)\right] + \mathcal{O}(R^4) \\ f^{\rm out}_2(r) &= \left[-\frac{1}{4} + \mathcal{O}(r^2)\right] + R^2\left[\frac{k+\frac{3}{4}}{r^2} + \mathcal{O}(r^0)\right] + \mathcal{O}(R^4) \\ A^{\rm out}_2(r) &= \left[-\frac{1}{8} + \mathcal{O}(r^2)\right] + R^2\left[\frac{4h_2+1}{4r^2} + \mathcal{O}(r^0)\right] + \mathcal{O}(R^4) \end{aligned} \tag{4.28}$$

4.3.2 Intermediate field region, $r \ll 1$ and $(r-R) \gg R^3$

As in the previous section, we find it convenient to work with the variables $y = \frac{r}{R}$ and $\tau = \frac{t}{R}$ in the intermediate field region. Recall also that, in these coordinates, the leading order metric has an overall factor of R^2. The metric variables that obey simple equations have this factor of R^2 stripped from them. For that reason we define Here

$$f^{\rm mid}(y) = \frac{g_{\tau\tau}}{R^2} = g_{tt} \quad \text{and} \quad g^{\rm mid}(y) = \frac{g_{yy}}{R^2} = g_{rr}$$

[19] At higher orders the same reasoning does not forbid singularities, but determines them in terms of the known intermediate field behaviour at one order lower.

JHEP11(2011)035

(here $g_{\mu\nu}$ are metric components. In a similar fashion we define $A^{\rm mid} = \frac{A_\tau}{R} = A_t$. With these definitions we expand

$$\begin{aligned} f_2^{\rm mid}(y) &= \sum_{k=0}^{\infty} R^{2k} f_{(2,2k)}^{\rm mid}(y) \\ g_2^{\rm mid}(y) &= \sum_{k=0}^{\infty} R^{2k} g_{(2,2k)}^{\rm mid}(y) \\ A_2^{\rm mid}(y) &= \sum_{k=0}^{\infty} R^{2k} A_{(2,2k)}^{\rm mid}(y) \end{aligned} \tag{4.29}$$

where

$$\begin{aligned} f_0^{\rm mid}(y) =& V(y), \qquad g_0^{\rm mid}(y) = \frac{1}{V(y)}, \qquad A_0^{\rm mid}(y) = \mu_0 \left(1 - \frac{1}{y^2}\right) \\ \mu_0 =& \sum_{k=0}^{\infty} R^{2k} \mu_{(0,2k)} \qquad \mu_{(0,0)} = 1, \qquad \mu_{(0,2)} = 0 \end{aligned} \tag{4.30}$$

The equations are slightly simpler when rewritten in terms of a new function

$$K_{(2,2k)}(y) = V_0(y) g_{(2,2k)}^{\rm mid}(y) + \frac{f_{(2,2k)}^{\rm mid}(y)}{V_0(y)}$$

where

$$V_0(y) = \left(1 - \frac{1}{y^2}\right)^2$$

In terms of this function the final set of equations take the form

$$\begin{aligned} \frac{dK_{(2,2k)}(y)}{dy} &= \text{Source} \\ \frac{d}{dy}\left(y^3 \frac{dA_{(2,2k)}^{\rm mid}(y)}{dy}\right) - \left(\frac{dK_{(2,2k)}(y)}{dy}\right) &= \text{Source} \\ \frac{d}{dy}\left(y^2 f_{(2,2k)}^{\rm mid}(y)\right) - 2y K_{(2,2k)}(y) + 2\left(\frac{dA_{(2,2k)}^{\rm mid}(y)}{dy}\right) &= \text{Source} \end{aligned} \tag{4.31}$$

These equations are all easily solved by integration, upto four undetermined integration constants (one each from the first and third equation, and two for the second). It will turn out that two of these constants are determined by matching with the far field solution while the other two are determined by matching with the near field solution. As in the previous section we will find that k^{th} order solutions scale like y^{2k} at large y, but scale like $\frac{1}{(z-1)^k}$ at small z.

The solution at leading order, R^0, is given by

$$\begin{aligned} f_{(2,0)}^{\rm mid}(y) &= \alpha_1 \left(1 - \frac{1}{y^2}\right) - \frac{2\alpha_2}{y^2} + \frac{2\alpha_3}{y^4} + \frac{\alpha_4}{y^2} \\ g_{(2,0)}^{\rm mid}(y) &= -\frac{\alpha_1 y^4}{(y^2-1)^3} - \frac{2\alpha_3 y^4}{(y^2-1)^4} + \frac{(2\alpha_2 - \alpha_4) y^6}{(y^2-1)^4} \\ A_{(2,0)}^{\rm mid}(y) &= \alpha_2 - \frac{\alpha_3}{y^2} \end{aligned} \tag{4.32}$$

JHEP11(2011)035

Here α_1, α_2, α_3 and α_4 are the four integration constants to be determined by matching.

Expanding (4.32) around $y = \infty$ one finds

$$\begin{aligned} f_2^{\rm mid}(y) &= \alpha_1 + \frac{(\alpha_4 - \alpha_1 - 2\alpha_2)}{y^2} + \mathcal{O}\left(\frac{1}{y^4}\right) + \mathcal{O}(R^2) \\ g_2^{\rm mid}(y) &= \frac{(2\alpha_2 - \alpha_1 - \alpha_4)}{y^2} + \mathcal{O}\left(\frac{1}{y^4}\right) + \mathcal{O}(R^2) \\ A_2^{\rm mid}(y) &= \alpha_2 - \frac{\alpha_3}{y^2} + \mathcal{O}(R^2) \end{aligned} \tag{4.33}$$

As usual, we substitute as $y = \frac{r}{R}$ and then match relevant terms of (4.33) and (4.28). This determines

$$\begin{aligned} \alpha_1 &= -\frac{1}{4} \\ \alpha_2 &= -\frac{1}{8} \\ h_2 &= -\left(\alpha_3 + \frac{1}{4}\right) \\ k &= \alpha_4 - \frac{1}{4} \end{aligned} \tag{4.34}$$

To facilitate matching with the near field region in the next subsection we expand $f_2^{\rm mid}(y)$, $g_2^{\rm mid}(y)$ and $A_2^{\rm mid}(y)$ about $y = 1$

$$\begin{aligned} f_2^{\rm mid}(y) =& \left[\left(\frac{1}{4} + 2\alpha_3 + \alpha_4\right) - (1 + 8\alpha_3 + 2\alpha_4)(y-1) + \left(\frac{3}{2} + 20\alpha_3 + 3\alpha_4\right)(y-1)^2 \right. \\ & \left. + \mathcal{O}\left((y-1)^3\right)\right] + \mathcal{O}(R^2) \\ g_2^{\rm mid}(y) =& \left[-\frac{1 + 8\alpha_3 + 4\alpha_4}{64(y-1)^4} - \frac{1 + 8\alpha_3 + 8\alpha_4}{32(y-1)^3} - \frac{1 + 8\alpha_3 + 44\alpha_4}{128(y-1)^2} \right. \\ & \left. + \mathcal{O}\left(\frac{1}{y-1}\right)\right] + \mathcal{O}(R^2) \\ A_2^{\rm mid}(y) =& -\left(\frac{1}{8} + \alpha_3\right) + 2\alpha_3(y-1) + \mathcal{O}\left((y-1)^2\right) + \mathcal{O}(R^2) \end{aligned} \tag{4.35}$$

4.3.3 Near field region $(r - R) \ll R$ or $(y - 1) \ll 1$

As in the previous section we work with the shifted and rescaled radial coordinate $z = \frac{y-1}{R^2}$. In this coordinate the black hole horizon is at $z = 0$. As we have seen in the previous section, g_{TT} and g_{rr} have an overall factor of R^2 even at leading order. For this reason the natural dynamical variables in the problem are

$$\frac{g_{TT}}{R^2} = \frac{g_{tt}}{R^4} \quad \text{and} \quad \frac{g_{zz}}{R^2} = R^4 g_{rr}$$

JHEP11(2011)035

(here $g_{\mu\nu}$ is the metric). For easy of matching with the intermediate field solution however, we will continue to use the notation

$$\begin{aligned} f^{\rm in} &= g_{tt} = R^4 \times \frac{g_{TT}}{R^2} \\ g^{\rm in} &= g_{rr} = \frac{1}{R^4} \times \frac{g_{zz}}{R^2} \\ A^{\rm in} &= A_t = R^2 \times \frac{A_T}{R} \end{aligned} \tag{4.36}$$

And so our perturbative expansion takes the form (note the lower limits of the sums)

$$\begin{aligned} f_2^{\rm in}(z) &= \sum_{k=2}^{\infty} R^{2k} f^{\rm in}_{(2,2k)}(z) \\ g_2^{\rm in}(z) &= \sum_{k=-2}^{\infty} R^{2k} g^{\rm in}_{(2,2k)}(z) \\ A_2^{\rm in}(z) &= \sum_{k=1}^{\infty} R^{2k} A^{\rm in}_{(2,2k)}(z) \end{aligned} \tag{4.37}$$

We now come to an important subtlety of our expansion procedure. First recall that the radial coordinate r employed in this paper has geometrical significance; it parametrizes the volume of the S^3 at that point. For this reason reparametrizations of r do not form a symmetry of the equations in this paper, in general. At leading order in the near field region, however, the metric metric takes the form

$$\frac{ds_0^2}{R^2} = -4z(1+z)dT^2 + \frac{dz^2}{4z(1+z)} + d\Omega_3^2 \tag{4.38}$$

Note in particular that the size of three sphere (at leading order) is a constant independent of z. For this reason the leading order metric equations in the near field region admit a whole functions worth (instead of 4 numbers worth) of solutions, parametrized by any $\mathcal{O}(\epsilon^2 R^0)$ redefinition of z coordinate. So without even doing any calculations, we have deduced that one linear combination of the three functions is undetermined at leading order.

Now let us move to the next order, $\mathcal{O}(R^2)$. As the homogeneous part of the equations are same at every order, the same linear combination of second order fluctuations disappears from (i.e. is undetermined by) the second order equations. However the 0 order 'gauge transformation' is now not a symmetry of the $\mathcal{O}(R^2)$ equations (because, at this order, we see the fact that the size of the sphere is not really constant). So the zero order 'gauge transformation function' shows up in the second order equations. As this term comes with an explicit R^2 (without this factor the equations cannot distinguish it from pure gauge) it cannot multiply any of the 2nd order unknowns, and so appears as a genuine unknown all by itself. The net upshot of all this is that at every order other than the leading, we actually do have as many equations as variables. The variables, however, consist of two unknown functions at that order coupled with the one unknown 'gauge transformation' at the previous order!

JHEP11(2011)035

We will now say all of this more precisely. Our equations can be simplified by performing the following redefinition of the functions (W is essentially the 'gauge transformation')

$$\begin{aligned} f^{\rm in}_{(2,2k)}(z) &= \frac{d}{dz}\left[4z(1+z)\right] W_{(2,2k)}(z) \\ g^{\rm in}_{(2,2k)}(z) &= \zeta_{(2,2k)}(z) + \frac{d}{dz}\left[\frac{1}{4z(1+z)}\right] W_{(2,2k)}(z) + \left[\frac{1}{2z(1+z)}\right]\frac{d}{dz}\left[W_{(2,2k)}(z)\right] \\ A^{\rm in}_{(2,2k)}(z) &= \chi_{(2,2k)}(z) + 2W_{(2,2k)}(z) \end{aligned} \tag{4.39}$$

In terms of these functions the equations at order R^{2k} take the form

$$\begin{aligned} \frac{d}{dz}\left[z(1+z)(1+2z)^2\zeta_{(2,2k)}(z)\right] &= \text{Source} \\ \frac{d}{dz}\left[\chi_{(2,2k)}(z)\right] - 4z(1+z)\zeta_{(2,2k)}(z) &= \text{Source} \\ \frac{d^2}{dz^2}\left[W_{(2,2k-2)}(z)\right] &= \text{Source} \end{aligned} \tag{4.40}$$

As we anticipated above, $W_{(2,2k)}(z)$ does not appear in the homogeneous equations at $\mathcal{O}(R^{2k})$ as at this order it is pure gauge. But it appears in the homogeneous equations of $\mathcal{O}(R^{2k+2})$. Therefore to completely determine the metric and gauge field (upto integration constants) at any given order R^{2k} , one has to solve one more equation at the order R^{2k+2} along with all the equations at order R^{2k}.

The equations (4.40) are completely well posed, and may easily be integrated to solve for $\zeta_{(2,2k)}(z)$, $\chi_{(2,2k)}(z)$ and $W_{(2,2k-2)}(z)$ in terms of four integration constants. Two of these constants are determined by the requirement that $f^{\rm in}_{(2,2k)}(z)$ and $A^{\rm in}_{(2,2k)}(z)$ vanish at the horizon $z = 0$. The remaining two constants are determined by matching with the intermediate range solution.

Solving the first two equations at $\mathcal{O}(R^0)$ and the third equation at $\mathcal{O}(R^2)$ one can find $\zeta_{(2,0)}(z)$, $\chi_{(2,0)}(z)$ and $W_{(2,0)}(z)$ respectively. The solution is the following.

$$\begin{aligned} \zeta_{(2,0)}(z) &= \frac{\Lambda_1}{z(1+z)(1+2z)^2} \\ \chi_{(2,0)}(z) &= \frac{4\Lambda_1 z}{1+2z} + \Lambda_2 \\ W_{(2,0)}(z) &= -\frac{\log[8(1+z)]}{8} + \frac{\Lambda_1}{1+2z} + z\beta_1 + \beta_2 \end{aligned} \tag{4.41}$$

Regularity at the horizon implies that

$$\Lambda_1 = \beta_2 + \frac{3\log 2}{8}, \quad \Lambda_2 = 0$$

After imposing the regularity at $z = 0$ the solution at the leading order

$$\begin{aligned} f^{\rm in}_{(2,4)}(z) &= -\frac{1}{2}(1+2z)\log(1+z) - 3(\log 2)z + 4\beta_1 z(1+2z) + 8\beta_2 z \\ g^{\rm in}_{(2,-4)}(z) &= \frac{1}{32z^2(1+z)^2}\left[(1+2z)\log(1+z) + 2z(3\log 2 - 1)\right] + \frac{\beta_1 - 2\beta_2}{4z(1+z)^2} \\ A^{\rm in}_{(2,2)}(z) &= -\frac{1}{4}\log(1+z) + 2z\beta_1 \end{aligned} \tag{4.42}$$

JHEP11(2011)035

Here β_1 and β_2 are the two constants which are to be determined by matching. Expanding around $z = \infty$ one finds

$$\begin{aligned} f_2^{\rm in}(z) &= R^4 \left[8\beta_1 z^2 + \mathcal{O}(z)\right] + \mathcal{O}(R^6) \\ g_2^{\rm in}(z) &= \mathcal{O}(R^{-2}) \\ A_2^{\rm in}(z) &= R^2 \left[2\beta_1 z + \mathcal{O}(z^0)\right] + \mathcal{O}(R^4) \end{aligned} \tag{4.43}$$

After substituting $z = \frac{y-1}{R^2}$ this expansion will match with (4.35) provided one chooses the constants in the following way

$$\begin{aligned} \alpha_3 &= -\frac{1}{8} \\ \alpha_4 &= 0 \\ \beta_1 &= -\frac{1}{8} \end{aligned} \tag{4.44}$$

In the whole solution at this order there are two constants left undetermined. The first is β_2 in the near field solution and the second is h_1 in the far field solution. In the expansion of $f_2^{\rm in}(z)$ the constant β_2 appears at $\mathcal{O}(R^4 z)$ which is equivalent to a term of $\mathcal{O}\left[R^2(y-1)\right]$ in expansion of $f_2^{\rm mid}(y)$. Therefore to compute this constant one needs the solution upto $\mathcal{O}(R^2)$ in the intermediate region. Upon determining this solution to $\mathcal{O}(R^2)$ one can solve for β_2 (as well as all the new constants appearing in the $\mathcal{O}(R^2)$ intermediate solution) in terms of h_1. It turns out that

$$\beta_2 = \frac{1}{16} + \frac{3}{8}\log 2 - \frac{h_1}{2}$$

So at the end the full solution to $\mathcal{O}(R^2)$ is determined in terms of a single constant, h_1, which in turn is determined only by the ϵ^3 order scalar field analysis. It turns out that

$$h_1 = 0$$

5 All spherically symmetric supersymmetric configurations

In this section we will analyze the set of spherically symmetric supersymmetric solutions of (1.2). The configurations we will find will include the solitons of section 3 (determined more simply than in that section), but will also include several solutions that are singular at the origin. In particular (as we have explained in the introduction) we will identify a one parameter set of singular supersymmetric solutions which we will conjecture to be physical; we will conjecture that these singular configurations may be obtained as the limit of nonsingular nonextremal solutions.

5.1 The equations of supersymmetry

The action (1.2) is a consistent truncation of $\mathcal{N} = 8$ gauged supergravity. Hence any solution of the equations of motion (2.10), which saturates the BPS bound $m = 3q$, corresponds to a supersymmetric solution of $\mathcal{N} = 8$ gauged supergravity and consequently of

JHEP11(2011)035

IIB SUGRA on $AdS_5 \times S^5$. Here we present a more direct analysis of the supersymmetry equations for the consistent truncation.[20]

The supersymmetry conditions in theories of this type have been analyzed in [15–17, 27]. In these works supersymmetric solutions were found for a more general truncation of $\mathcal{N} = 8$ supergravity to $\mathrm{U}(1)^3$ gauged supergravity coupled to 3 hypermultiplets. Our theory is a special case of theirs where all three U(1) charges and three hyperscalars are taken to be equal. Specializing their results to our theory we find that spherically symmetric supersymmetric configurations can be written as follows. The metric, gauge field and scalar are[21]

$$\begin{aligned} ds^2 &= -\frac{1+\rho^2 h^3}{h^2}\, dt^2 + \frac{h}{1+\rho^2 h^3}\, d\rho^2 + \rho^2\, h\, d\Omega_3^2 \\ A &= h^{-1} dt, \qquad\qquad \phi = 2\sqrt{(h+\rho h'/2)^2 - 1} \end{aligned} \tag{5.1}$$

The entire solution is then determined by the single function $h(\rho)$ which is constrained to satisfy the following ordinary differential equation

$$(1+\rho^2\, h^3)\left(3\, h' + \rho\, h''\right) = \rho\left[4 - \left(2\, h + \rho\, h'\right)^2\right] h^2 \tag{5.2}$$

Notice that prime denotes differentiation with respect to the variable ρ.

This parametrization of the metric is somewhat different from the one that we used in the previous section, so we explain how the two are related. Comparing the coefficient of $d\Omega_3^2$ in the metric (5.1) to that of (2.9) we see that the two radial coordinates are related by

$$r^2 = \rho^2\, h(\rho) \tag{5.3}$$

Comparing the other coefficients of the two metrics we find

$$f(r) = \frac{1+\rho^2 h^3}{h^2} \qquad , \qquad g(r) = \frac{4\rho^2 h^2}{(2\rho h + \rho^2 h')^2 (1+\rho^2 h^3)} \tag{5.4}$$

With these identifications it is a matter of algebra to verify that equation (5.2) is sufficient for the equations of motion (2.10) to be satisfied.

[20] Let us first briefly describe how one could supersymmetrize the action (1.2). The bosonic field content of our theory is that of minimal gauged supergravity (i.e. the graviton and the U(1) gauge field) coupled to matter (the charged scalar ϕ). The scalar field can be thought of as a member of a hypermultiplet. A complete hypermultiplet would contain 2 complex scalar fields. Therefore, to supersymmetrize the action (1.2) we have to add one more scalar field, besides the fermions, and the resulting theory is minimal gauged supergravity coupled to a hypermultiplet. However, in the set of solutions that we are interested in, the additional scalar field can be consistently set to zero so we can ignore it in what follows.

[21] Let us explain our notation in relation to the notation of [16]. We have: $r_{there} = \rho_{here}$, $(H_1)_{there} = (H_2)_{there} = (H_3)_{there} = h_{here}$, $A_{there} = -A_{here}$, $2\sinh(\phi_{there}) = \phi_{here}$.

JHEP11(2011)035

In summary the most general spherically symmetric supersymmetric solutions to the equations of motion (2.10) is given by the configuration

$$\begin{aligned} g(r) &= \frac{4\rho^2 h^2}{(2\rho h + \rho^2 h')^2 (1+\rho^2 h^3)} \\ f(r) &= \frac{1+\rho^2 h^3}{h^2} \\ A(r) &= \frac{1}{h(r)} \\ \phi(r) &= 2\sqrt{(h+\rho h'/2)^2 - 1} \end{aligned} \tag{5.5}$$

with

$$r^2 = \rho^2 h(\rho) \tag{5.6}$$

and $h(\rho)$ any function that obeys (5.2).

5.2 Classification of supersymmetric solutions

As we have explained in the previous subsection, supersymmetric solutions to the equations of motion are given by solutions to the second order differential equation

$$(1+\rho^2\, h^3)\left(3\, h' + \rho\, h''\right) = \rho\left[4 - \left(2\, h + \rho\, h'\right)^2\right] h^2 \tag{5.7}$$

In this paper we are only interested in regular normalizable solutions to these equations. It is of crucial importance to this section that the condition of normalizability is automatically met; an analysis of (5.2) at large ρ immediately reveals that *all* solutions to this equation behave at large ρ like[22]

$$h(\rho) = 1 + \frac{2q}{\rho^2} + \ldots$$

ensuring normalizability for all physical fields.[23] The importance of this observation is the following; one may study the small ρ behaviour of supersymmetric solutions in a purely local manner, without having to worry about when the solutions we study have acceptable large ρ behaviour, as that is always guaranteed. This fact allows us, in this section, to use local analysis to present a simple classification of normalizable supersymmetric solutions. Relatedly, supersymmetric solutions may be obtained by solving (5.2) as an initial value problem with initial conditions set at small ρ. This is numerically and conceptually simpler than the boundary value problem we would have to solve by shooting methods off supersymmetry.

[22] Using (5.3) and (5.1) we find that this implies the large r behavior of the gauge field

$$A(r) = 1 - \frac{2q}{r^2} + \ldots$$

so the constant q may be identified with the electric charge of the solution, in the conventions of previous sections.

[23] This fact has a natural explanation from the viewpoint of the dual $\mathcal{N} = 4$ Yang Mills field theory; a deformation of the Lagrangian of that theory by only mass term $TrX^2 + TrY^2 + TrZ^2$ preserves no supersymmetry.

JHEP11(2011)035

It remains to impose the condition of 'regularity'. Let us first explain what we mean by this term. We call a supersymmetric configuration 'regular' if it can be regarded as the limit of a one parameter set of smooth nonsupersymmetric (and so non extremal) solutions to the equations of motion (2.10). While every smooth supersymmetric solution is automatically 'regular', a singular susy solution may also be 'regular', if its singularity can be removed upon heating the solution up infinitesimally.

Solutions to (5.2) can develop singularities only at $\rho = 0$. In this subsection we will classify all possible behaviours of solutions to (5.2) near $\rho = 0$. In a later subsection we will then go on to present conjectures about which of these solutions are 'regular'.

In order to investigate possible behaviours of solutions to (5.2) at small ρ we plug in the ansatz $h(\rho) = \frac{A}{\rho^\alpha}$ into the equation. It is easy to check that the only values of α that solve the equation near $\rho = 0$ are $\alpha = 0, \frac{2}{3}, 1, 2$. It is also possible to demonstrate (see below) that there is a unique solution with $\alpha = \frac{2}{3}$. On the other hand solutions with $\alpha = 0$ and $\alpha = 1$ both appear in a one parameter family. Finally, the generic solution to the differential equation has $\alpha = 2$; solutions with $\alpha = 2$ appear in a 2 parameter family.[24]

5.2.1 $h(\rho) \approx \rho^{-\frac{2}{3}}$

As we have mentioned above, there is a unique solution with $\alpha = \frac{2}{3}$. This solution may be expanded at small ρ as follows

$$h(\rho) = \rho^{-2/3} + \frac{9}{26}\rho^{2/3} - \frac{243}{20956}\rho^2 + \mathcal{O}(\rho^{8/3}) \tag{5.8}$$

We now present a crude estimate for validity domain of the expansion (5.8). Note that the formal procedure that generates the series expansion (5.8) treats the term proportional to 4 (in the r.h.s. of (5.2)) as subleading to the term proportional to h. This procedure is valid whenever $\rho \ll 1$; as a consequence we expect the expansion (5.8) to be valid whenever $\rho \ll 1$ but to break down at larger values of ρ.

For $\rho \ll 1$ the metric, gauge field and scalar corresponding to this solution take the following form

$$\begin{aligned} ds^2 &\approx -2r^2dt^2 + \frac{9}{8}dr^2 + r^2 d\Omega_3^2 \\ A(r) &\approx r dt \\ \phi(r) &\approx \frac{4}{3r} \end{aligned} \tag{5.9}$$

where we used the relations (5.5) and (5.6) to bring the solution in the form of (2.9).

We will denote the distinguished singular solution of this subsection by S. We will now explain that there is a sense in which S is a fixed point of the equation (5.2) viewed as a flow equation in the variable $\log \rho = x$ (see [29–31] for similar discussions in distinct but similar contexts). For this purpose we redefine

$$h(\rho) = e^{-\frac{2}{3}x} f(x)$$

[24] One special exact solution of (5.2) is $h(\rho) = 1 + \frac{q}{\rho^2}$, the so-called "superstar" [28]. This solution has $\alpha = 2$. For this solution we notice that the scalar field is not turned on ($\phi = 0$). So in a sense it is qualitatively different from the "hairy" configurations of interest to us in this paper.

JHEP11(2011)035

The differential equation (5.2) becomes

$$9f''(1+f^3)+3f'(2+3f^2f'+10f^3)+8(f^4-f)-36e^{4x/3}f^2=0$$

For very small ρ (that is for $x\to-\infty$) the last term in the equation can be ignored, and the equation becomes approximately time translation invariant (or an autonomous equation, in the language of dynamical systems). With this approximation the system has an exact solution $f(x)=1$, which is precisely the leading small ρ approximation to the solution S. We will restrict attention to large negative values of x in the rest of this subsubsection, and so study the truncated equation

$$9f''(1+f^3)+3f'(2+3f^2f'+10f^3)+8(f^4-f)=0 \tag{5.10}$$

Let us consider a small perturbation about $f=1$, i.e. we set

$$f(x)=1+\varepsilon g(x). \tag{5.11}$$

To linear order in ε the (5.10) turns into the linear ODE

$$3g''+6g'+4g=0 \tag{5.12}$$

The two linearly independent solutions to this equation are

$$\begin{aligned} g(x)&=e^{\lambda x}\\ \lambda&=-1\pm\frac{i}{\sqrt{3}} \end{aligned} \tag{5.13}$$

Note that the real part of the each of these eigenvalues is negative, which demonstrates that $f=1$ is a stable fixed point of the dynamical system (5.10). Moving back to the variable ρ, it follows that arbitrary small perturbations around the solution S behaves like

$$h(\rho)\approx\rho^{-2/3}\left(1+\varepsilon\frac{1}{\rho}\cos\left(\frac{1}{\sqrt{3}}\log\rho+a\right)\right)$$

Note that all perturbations die out for $\rho\gg\epsilon$ (this is a restatement of the fact that $f=1$ is a stable fixed point).

5.2.2 $h(\rho)\approx h_o+\mathcal{O}(\rho^2)$

We now turn to regular solutions to (5.2), i.e. solutions with $\alpha=0$. Such solutions appear in a one parameter set, labeled by $h_0=h(0)$. The small ρ expansion of (5.2) is given by

$$h(\rho)=h_0+\frac{1}{2}(h_0^2-h_0^4)\rho^2+\frac{1}{6}(h_0^3-5h_0^5+4h_0^7)\rho^4+\mathcal{O}(\rho^6) \tag{5.14}$$

The solutions of this subsection are simply the solitons studied in section 3. These solutions were generated perturbatively (i.e. at h_0-1 small) in section 3.

Let us now turn to the opposite limit of large h_0. Let us first inquire as to the validity domain of the expansion (5.14). As the term $h^3\rho^2$ on the l.h.s. of (5.2) is of order ρ^2, the formal process that generates the power series expansion (5.14) treats this

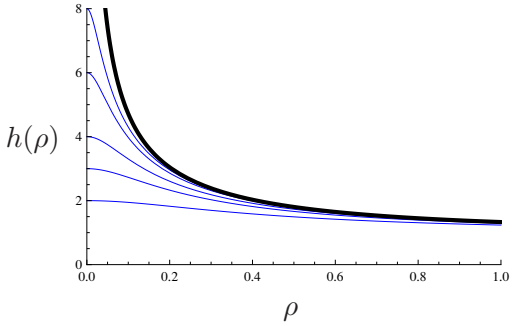

Figure 3. Convergence of the numerical solutions for the regular solitons to the special singular solution S as we increase $h_0 = h(0)$. The black line corresponds to the solution S with $\rho^{-2/3}$ behavior near $\rho = 0$. The blue lines correspond to regular solitons of $h_0 = 2, 3, 4, 6, 8$, starting from the lowest blue curve and going up.

term as subleading compared to unity. This is actually correct only when $h_0^3\rho^2 \sim 1$. It follows that when h_0 is large the series expansion (5.14) will break down at the small value $\rho \sim \rho_{rb} \sim h_o^{-\frac{3}{2}}$.

When h_0 is large, the expansion (5.14) does not apply in the range $\rho \gg h_o^{-\frac{3}{2}}$. If $\rho \ll 1$ in this range, however, the general arguments presented above guarantee that our solution behaves like $\rho^{-\alpha}$ for one of the allowed values of α described above. What solution does the expansion (5.14) match onto in this range? A clue to the answer to this question is given by noting that the value of $h(\rho)$, at the point of break down of (5.14) is approximately given by $h_0 \sim \rho_{rb}^{-\frac{2}{3}}$. Thus the solution (5.14) could smoothly match onto the special solution S of previous subsubsection, at $\rho \sim \rho_{rb}$. This suggests that the special solution S of the previous subsubsection is the limit as $h_0 \to \infty$ of the solutions of this subsubsection. We now present numerical evidence that strongly supports this guess. In figure (3) we present numerically generated plots of the regular solution parametrized by h_0 for successively increasing values of h_0. Note that, as h_0 increases, the entire profile of the solution approaches a limiting shape, with a sharp spike near $\rho = 0$. The spike becomes sharper as we increase h_0, while the solution at larger values of ρ remains almost unchanged. The limiting solutions indeed appears to be the special solution S of the previous subsubsection (denoted by the solid line in figure 3). Thus it appears that the solution S forms the end point of the family of regular supersymmetric solitons.

We will now study in more detail how solutions with large h_0 approach the special solution S. We work in the language of the dynamical system (5.10). We are given a function $f(x)$ that starts out, at large negative values of x (small ρ) as

$$f(x) = h_0 e^{\frac{2x}{3}} \left(1 + \mathcal{O}(e^{2x})\right) . \tag{5.15}$$

We wish to study how $f(x)$ evolves under (5.10) at later times. We are interested in the limit in which h_0 is large; as we have argued above, we expect $f(x)$ to increase to a value of order unity at a time $x_0 \sim -\frac{3}{2}\ln h_0$, and thereafter stabilize exponentially to the fixed point $f = 1$. Note that $x_0 \ll -1$ (this follows because of our assumption that h_0 is large) ,

JHEP11(2011)035

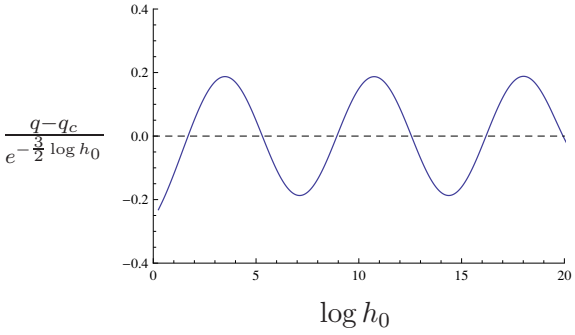

Figure 4. The damped oscillations of q around the critical value q_c for large h_0.

so that f should settle down to very near unity well within the domain of applicability of the dynamical system (5.10).[25]

Let us now compute $f(x_1)$ for some fixed (h_0 independent) x_1 that obeys[26]

$$x_0 \ll x_1 \ll -1.$$

In order to do this we recall that the equation (5.10) is invariant under translations in x. Now the judiciously chosen translation

$$x' = x + \frac{3\ln h_0}{2}$$

eliminates the h_0 dependence of the initial condition (5.15) . Let $\chi(x)$ be the (unique, h_0 independent) solution to (5.10) that reduces at early (large negative) times to $\chi(x') = e^{\frac{2x'}{3}}$. It follows that the solution of interest to us is

$$f(x) = \chi\left(x + \frac{3\ln h_0}{2}\right).$$

The key assumption of this section, is that the function χ lies within the domain of attraction of the fixed point $f = 1$ (as we have seen above there is impressive numerical evidence for this assumption). If this is the case it follows from (5.11) and (5.13) that at large x' (i.e. for $x \gg x_0$;)

$$\chi(x') = 1 + Ae^{-x'}\cos\left(\frac{x'}{\sqrt{3}} + \delta\right)$$

for some unknown, order unity constants A and δ. It follows that

$$f(x_1) \approx 1 + Ae^{-\frac{3}{2}\log h_0 + x_1}\cos\left(\frac{\sqrt{3}}{2}\log(h_0 + x_1) + \delta\right) \tag{5.16}$$

Of course the x_1 dependence of this result may be absorbed into a redefinition of A and δ.

[25] In this language, the conjecture of the previous paragraph is equivalent to the assumption that this fluctuation lies within the domain of attraction of the fixed point $f = 1$.

[26] Recall that (5.10) is valid only for large and negative x_1.

Let $\rho_1 = e^{x_1}$. (5.16) gives us a formula for $h(\rho_1)$ and $h'(\rho_1)$ for the solution of interest; these values may be used as an 'initial conditions' to generate $h(\rho)$ for all $\rho > \rho_1$. The resultant solution will take the form

$$h(\rho) \approx h_S(\rho) + \delta h(\rho)$$

where $h_S(\rho)$ is the special solution S and $\delta h(\rho)$ is a small fluctuation (of order $\sim \mathcal{O}(\frac{1}{h_0^{\frac{3}{2}}})$) about this solution. To leading order in this small parameter, the function $\delta h(\rho)$ obeys a linear differential equation, and so depends linearly on $h(\rho_1)$ and $h'(\rho_1)$. It follows that (5.16) then determines the behaviour of every observable (like the charge) of the solution that depends only on the behaviour of $h(\rho)$ for ρ of order unity or greater. In particular it follows that the dependence of the charge of solutions on h_0 is given approximately by

$$q(h_0) \approx q_c + A e^{-\frac{3}{2}\log h_0} \cos\left(\frac{\sqrt{3}}{2}\log h_0 + \delta\right) \tag{5.17}$$

for some constants A, δ. While A and δ can only be determined numerically, we have a sharp analytic prediction for the form (5.17). A similar formula applies for the vacuum expectation value of the operator dual to ϕ as a function of h_0.

We have verified the prediction (5.17) numerically; in figure 4 we present a plot of the rescaled oscillations of q about q_c. This graph displays precisely the damping (reflected in the h_0 dependent renormalization of the y axis in figure 4) and the oscillations predicted by (5.17). We will give more details below.

5.2.3 $h(\rho) \approx \frac{a}{\rho}$

Next we consider solutions with $\alpha = 1$, i.e solutions that behave near $\rho = 0$ like $\frac{a}{\rho}$. The one parameter set of these solutions may be labeled by a. At small ρ our solution takes the form $\frac{a}{\rho}P(\rho)$ where $P(\rho)$ is a regular power series. The first few terms in the power series expansion are given by

$$h(\rho) = \frac{1}{\rho}\left(a + \frac{1}{3a^2}\rho + \frac{18a^4 - 5}{36a^5}\rho^2 + \frac{-90a^4 + 31}{270a^8}\rho^3 + \mathcal{O}(\rho^4)\right) \tag{5.18}$$

The formal procedure that generates the power series (5.18) treats the term proportional to unity (on the l.h.s. of (5.2)) as subleading compared to the term proportional to $h^3\rho^2$. When $a \ll 1$, this is justified only when $\rho \ll a^3$. Consequently we expect the expansion (5.18) to break down at $\rho_{sb} \sim a^3$.

As in the previous subsubsection, the solution presented here must reduce to one of the other solutions of this section when $a^3 \ll \rho \ll 1$. Noting that, at the point of breakdown of (5.18), the function h may be estimated by $h \sim \frac{1}{a^2} \sim \rho_{sb}^{-\frac{2}{3}}$, it is natural to guess that the solution of this subsubsection tends to the special solution S in the limit of small a. We now present strong numerical evidence in support of this guess. In figure (5) we present numerical plots of the solution of this subsection for a range of decreasing values of a. Note that the solution converges to the solution S (denoted by the solid line in figure (5)) at small a.

JHEP11(2011)035

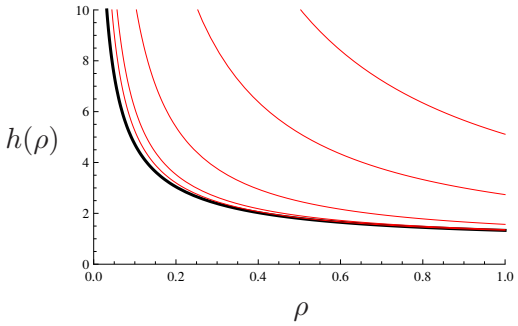

Figure 5. Convergence of the numerical solutions for singular solitons with an $\frac{a}{\rho}$ singularity to the special singular solution S as we decrease a. The black line corresponds to the solution S with $\rho^{-2/3}$ behavior near $\rho = 0$. The red lines correspond to singular solitons of $a = 0.35, 0.5, 1, 2.5, 5$, starting from the lowest red curve and going up.

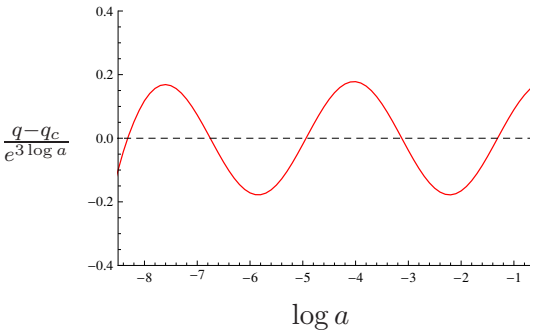

Figure 6. The damped oscillations of q around the critical value q for small a.

For $\rho \ll 1$ the metric, gauge field and scalar corresponding to this solution take the following form

$$\begin{aligned} ds^2 &\approx -r^2 dt^2 + \frac{4r^2}{a^4} dr^2 + r^2 d\Omega_3^2 \\ A(r) &\approx \frac{r^2}{a^2} dt \\ \phi(r) &\approx \frac{a^2}{r^2} \end{aligned} \tag{5.19}$$

Precisely as in the previous subsubsection, we can analytically study the approach of the solution with small a to the solution S. Repeating an analysis very similar to that of the previous subsubsection, we conclude that the dependence of, for instance, the charge of the solution on a is given by the formula

$$q(h_0) \approx q_c + A e^{3\log a} \cos\left(\sqrt{3}\log a + \delta\right)$$

for some constants A, δ which cannot be determined analytically. We have verified this prediction numerically (see figure 6). A similar formula applies for the vacuum expectation value of the operator dual to the field ϕ, as a function of h_0.

JHEP11(2011)035

5.2.4 The generic solution, $\alpha = 2$

Finally we move to the case $m = 2$. Now we find a two parameter set of solutions, labeled by two arbitrary constants a, b, which have the form

$$h(\rho) = \frac{1}{\rho^2}\left[a + \frac{1-b^2}{2a}\,\rho^4 - \frac{(b^2-1)(3a(5b^2-1)-2)}{24a^4}\,\rho^8 + \mathcal{O}(\rho^{12})\right] \tag{5.20}$$

The value $b = 1$ is special; as we have already remarked $h = 1 + \frac{a}{\rho^2}$ is an exact solution; hints of this fact are already visible in the expansion (5.20). It follows in particular that the values $b = 1$ lies outside the basin of attraction of the fixed point S at least when $b = 1$. A very rudimentary numerical investigation suggests that this is also true for all values of a at (for example) $b = 2$. Although we have not carefully investigated this question, it seems possible that the solutions with $\alpha = 2$ are completely disconnected from all the other solutions studied above.

For the reasons outlined in the previous paragraph, the 'generic' solutions of this subsubsection will make no further appearance in our paper. We suspect that all — or at least most — of these solutions are genuinely singular, in the sense that they cannot be regarded as the limit of smooth solutions. We leave a fuller study of these solutions, and their possible physical significance, to future work.

5.3 'Regular' supersymmetric solutions

In this section we present the results of a numerical analysis of the space of 'regular' supersymmetric solutions. Let us first describe what we believe the space of these solutions to be. The smooth supersymmetric solitons (with $\alpha = 0$) of the previous subsection are clearly regular. However this space of solutions ends at finite charge (see below) as $h_0 \to \infty$. As we have described above, this line of solutions spirals into (and ends in) the special solution S. We have also seen above that another line of solutions — those with $\alpha = 1$ and small values of a — spiral out of the solution S. As we will see below, the charge of this new line of solutions increases without bound at large a. It thus seems that the solutions with $\alpha = 0$ and $\alpha = 1$ may be regarded as two different segments of a single line of supersymmetric solutions. The two segments are joint together (by a very intricate non intersecting double spiral structure) at the special solution S. At least one member of this line of solutions exists at every value of the charge, and so constitutes a candidate end point of the phase diagram figure 2. We conjecture that it is indeed the case that hairy black holes at every value of the charge exist for all energies above the BPS bound. In the BPS limit, these solutions reduce to some configuration on this special line of solutions; either to the smooth supersymmetric soliton (at small charges) or the $\alpha = 1$ solutions (at large charges). In particular we conjecture that all solutions on the special line described in this are 'regular', where this word is used in the sense specified in the previous subsection. We now proceed to study these conjecturally regular solutions in more detail.

JHEP11(2011)035

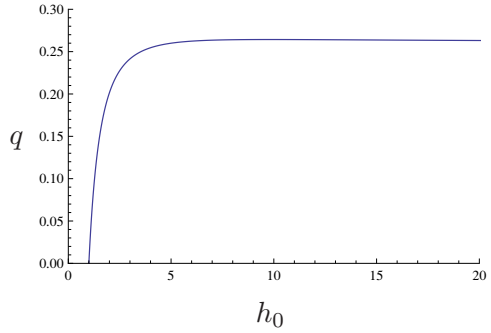

Figure 7. Charge q of spherically symmetric supersymmetric regular solitons as a function of the value $h_0 \equiv h(0)$.

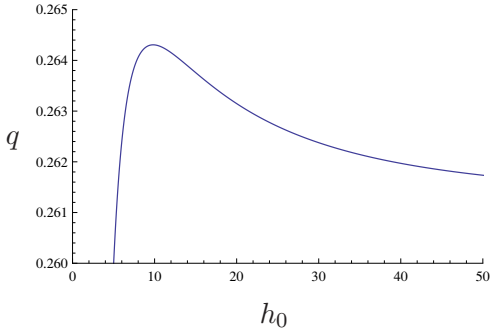

Figure 8. The same graph with different scales on the axes, where we can see the maximum charge.

5.3.1 Solitons

We first present the numerical analysis of regular solutions of (5.2). For this we fix the initial conditions $h(0) = h_0 \geq 1$[27] and $h'(0) = 0$ and integrate the equation outwards. For each value of h_0 we compute the solution $h(\rho)$ numerically and we evaluate the charge $q(h_0)$. The results can be seen in figures 7, 8 and 9, in various magnifications.[28]

The most striking feature of the numerical analysis is the existence of a maximum value[29]

$$q_{\max} \approx 0.2643 \tag{5.21}$$

for the charge of regular supersymmetric solitons. This charge is obtained for the value $h_{q_{\max}} \approx 9.821$ of the initial conditions at the center. The existence of a maximum charge for these solitons was also noticed in [16].[30] For higher values of h_0 the charge of the solution

[27]The condition $h_0 \geq 1$ is necessary since the scalar field at $\rho = 0$ is given by $\phi(0) = 2\sqrt{h_0^2 - 1}$ and has to be real by assumption (2.9).

[28]To partly check the validity of the numerics it is easy to perform a perturbative analysis of equation (5.2), similar to that of the previous sections i.e. in a small amplitude of $h(\rho) - 1$. One finds agreement between numerics and perturbation theory (i.e. convergence of the perturbative solution to the numerical one, for small enough values of $h_0 - 1$). Notice that the case $h_0 = 1$ is precisely empty AdS.

[29]We have solved the equations numerically using Mathematica.

[30]Notice that we are working in slightly different conventions from [16], in which $q_{there} = 2q_{here}$. This is consistent with the maximum charge $(q_m)_{there} = 0.529$ reported in that paper.

JHEP11(2011)035

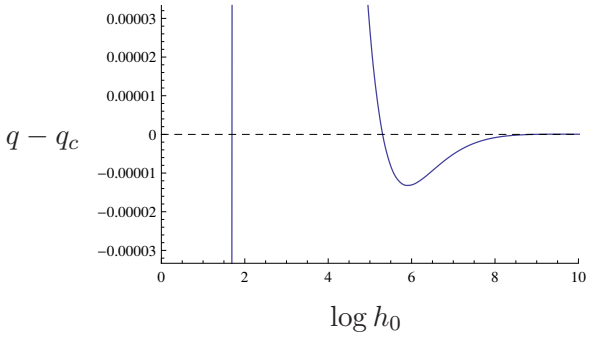

Figure 9. Magnification of the previous graph. We wee the next oscillation around q_c.

starts to decrease and asymptotically it approaches the limiting value

$$q_c \approx 0.2613 \tag{5.22}$$

as $h_0 \to \infty$.

A more careful analysis reveals that the convergence of the function $q(h_0)$ towards the critical value q_c is not monotonic. Instead, the function $q(h_0)$ undergoes slow oscillations around the critical value, as can be seen in figure 9 and in more detail in figure 4. These oscillations are periodic, with damped amplitude, if expressed in terms of $x = \log h_0$. As we explained in section 5.2.2 the asymptotic form of these oscillations can be determined analytically by matching the regular solution for large h_0 to the special $\rho^{-2/3}$ solution S and we have the following asymptotic formula for large h_0

$$q(h_0) \approx q_c + Ae^{-\gamma \log h_0} \cos(\omega \log h_0 + \delta) \tag{5.23}$$

In section 5.2.2 we saw that the period of the oscillations and the damping constant can be determined analytically from the matching procedure to be

$$\gamma = 3/2, \quad \omega = \sqrt{3}/2. \tag{5.24}$$

while A and δ cannot be fixed in this way. If one tries to fit this formula to the numerical data one finds

$$\gamma \approx 1.50, \qquad \omega \approx 0.87, \qquad A \approx -0.19, \qquad \delta \approx 0.12 \tag{5.25}$$

which are in very good agreement with the exact values.

The number of regular solitonic solutions as a function of the charge are as follows: for small enough charge there is only one solution. As we increase the charge, at some point we hit the first oscillation around q_c, which increases the number of solutions to three. Increasing q further we encounter the second oscillation and we have five solutions, and so on. As we approach the critical value q_c from below the number of solutions is always an odd integer which goes to infinity. Now let us consider the large charge behavior. For $q > q_{\max}$ we have no regular solitonic solution. As we decrease the charge and we go below $q_{\max}$ we first find two solution. As we decrease further we encounter the first oscillation

JHEP11(2011)035

above q_c, giving us four solutions, then the second oscillation to six solution and so on. Hence for $q > q_c$ we always have an even number of solutions (possibly zero) which tends to infinity as we approach q_c from above.

Notice that since the BPS bound $m = 3q$ is satisfied for all of these solutions, the figures 7, 8 also show the dependence of the mass of the solution on the value of the field at the center. This qualitative behavior, i.e. the existence of a maximum mass, and of a slightly lower critical value of the mass which is approached asymptotically for large central density via a function which undergoes damped oscillations, is typical in related problems in general relativity [32–34].[31] To our knowledge, however, this is the first time such behaviour has been observed in family of supersymmetric solutions.

Let us now study the expectation value of the scalar operator dual to ϕ, which we denote by $\langle \mathcal{O}_\phi \rangle$, as a function of h_0. Since $\mathcal{O}_\phi$ is an operator of dimension $\Delta = 2$, its expectation value can be determined from the large r expansion of ϕ as

$$\phi(r) = \frac{\langle \mathcal{O}_\phi \rangle}{r^2} + \dots$$

We plot the results in figures 16, 17, 18 in appendix C. The qualitative behavior is similar to that of the charge q: the expectation value $\langle \mathcal{O}_\phi \rangle$ is an increasing function of h_0 up to a maximum value

$$\langle \mathcal{O}_\phi \rangle_{\max} \approx 1.8906 \tag{5.26}$$

which is realized for $h_0 \approx 6.580$ and then decreases and approaches the asymptotic value

$$\langle \mathcal{O}_\phi \rangle_c \approx 1.8710 \tag{5.27}$$

as $h_0 \to \infty$, while performing small oscillations around it. Again the oscillations can be determined following the logic of section 5.2.2 and are captured by the formula

$$\langle \mathcal{O}_\phi \rangle(h_0) \approx \langle \mathcal{O}_\phi \rangle_c + A e^{-\gamma \log h_0} \cos\left(\omega \log h_0 + \delta\right) \tag{5.28}$$

The analytic prediction is $\gamma = \frac{3}{2}$, $\omega = \frac{\sqrt{3}}{2}$. If one tries to fit this formula to the numerical data one finds

$$\gamma \approx 1.50, \qquad \omega \approx 0.87, \qquad A \approx -0.66, \qquad \delta \approx 0.48 \tag{5.29}$$

which are in good agreement with the exact values.

Before we proceed let us point out that the value of h_0 at which we have the maximum charge ($h_{q_{\max}} \approx 9.821$) differs from the one at which we have the largest expectation value

[31] Generally, when a family of gravitational solutions has the property that their mass has a local maximum for some value of the initial conditions at the center, it is the sign that one of the two branches (to the left or right of the local maximum) is unstable (under radial perturbations) and thus unphysical. This is the analogue of the "Chandrasekhar instability": if we expand the equations of motion around the solution at the local maximum of the mass they have a zero mode, since the total mass does not change to first order in the perturbation. Generically this zero mode will be stable on one side and unstable (i.e. tachyonic) on the other side of the local maximum. This is what happens for example in the case of boson stars [35]. In our case the solutions are supersymmetric for all values of h_0. It would be very interesting to check what this implies about their stability.

JHEP11(2011)035

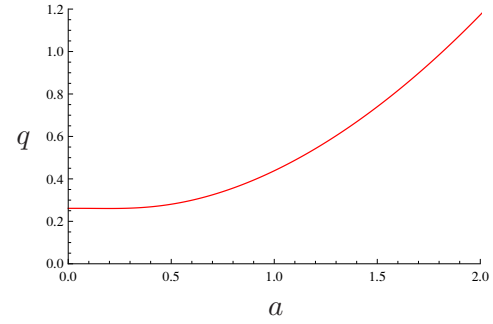

Figure 10. Charge q of spherically symmetric supersymmetric solitons with a singularity of the form $\frac{a}{\rho}$ at $\rho = 0$.

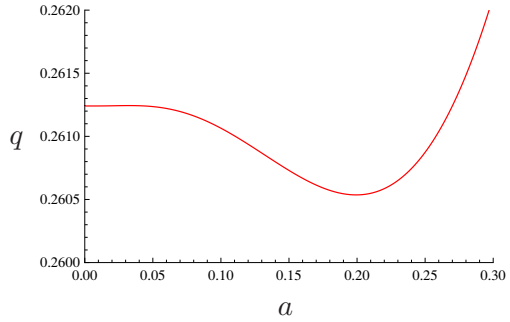

Figure 11. Detail of the previous graph with different scales on the axes, where we can see the minimum of the charge near $a = 0$.

$\langle \mathcal{O}_\phi \rangle_{\max}$, which turns out to be $h_{\langle \mathcal{O}_\phi \rangle_{\max}} \approx 6.580$. More generally, and as we will see more clearly in subsection 5.4, while there are pairs of regular solitonic solutions with the same charge q or the same expectation value $\langle \mathcal{O}_\phi \rangle$, there are no such pairs which have the same q and same $\langle \mathcal{O}_\phi \rangle$ simultaneously.

5.3.2 Solutions with $\alpha = 1$

We now present the results of a numerical investigation of the other segment of the line of (conjecturally) 'regular' supersymmetric solutions: those whose small ρ behaviour is given by a/ρ for small ρ. We compute the entire solution numerically and calculate the charge q as a function of a. The results are shown in figures 10, 11, 12. As we see in the figures the charge of this family starts (at small a) precisely at the point $q = q_c$ (5.22) where the family of regular solitons ended, then as we increase a the charge seems to decreases, down to a minimum value

$$q_{\min} = 0.2605 \tag{5.30}$$

and then increases all the way to arbitrarily large values.

As before, a more careful analysis shows that the entire radial profile of solutions with $\frac{a}{\rho}$ singularities converges to the special solution S in the limit $a \to 0$, as shown in figure 5. Again, a closer inspection shows that in the regime between $a = 0$ and the point where $q = q_{\min}$ the function $q(a)$ is not monotonically decreasing, but rather is undergoing small

JHEP11(2011)035

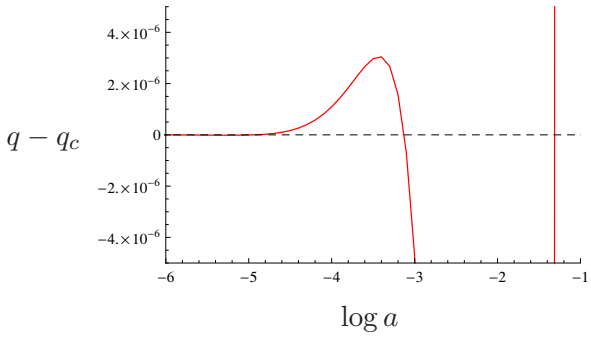

Figure 12. Magnification of the previous graph. We wee the next oscillation around q_c.

damped oscillations around the value q_c as a function of $\log a$. This is shown in figure 6. For small values of a the form of these oscillations can be determined by the matching procedure discussed in section 5.2.3 and we find the following formula

$$q(a) \approx q_c + Ae^{\gamma \log a} \cos(\omega \log a + \delta) \tag{5.31}$$

with the analytically determined values (see 5.2.3) $\gamma = 3$, $\omega = \sqrt{3}$. From the numerics we find

$$\gamma \approx 3.00, \qquad \omega \approx 1.73, \qquad A \approx 0.18, \qquad \delta \approx 0.70 \tag{5.32}$$

which are in good agreement with the exact values.

We find similar behavior for the expectation value $\langle \mathcal{O}_\phi \rangle$ as shown in figures 20, 21 in appendix C: the expectation value starts at the point (5.27) where the regular soliton family ended, it then goes down to

$$\langle \mathcal{O}_\phi \rangle_{\min} \approx 1.8658 \tag{5.33}$$

and then increases indefinitely.

Finally we have the following oscillatory behavior for small a which is shown in figure 23

$$\langle \mathcal{O}_\phi \rangle(a) \approx \langle \mathcal{O}_\phi \rangle_c + Ae^{\gamma \log a} \cos\left(\omega \log a + \delta\right) \tag{5.34}$$

with the exact values $\gamma = 3$, $\omega = \sqrt{3}$. From the numerics we find

$$\gamma \approx 2.97, \qquad \omega \approx 1.74, \qquad A \approx 0.59, \qquad \delta \approx -0.34 \tag{5.35}$$

Let us mention that the numerical results depicted in figure 14 agree with the perturbative analysis of section 3 in the regime of small q. According to the results of that section we expect that for small q the expectation value $\langle \mathcal{O}_\phi \rangle$ goes like

$$\langle \mathcal{O}_\phi \rangle = 4\sqrt{q} + \dots$$

One can indeed verify that the small q behavior of the curve in figure 14 agrees with this result.

JHEP11(2011)035

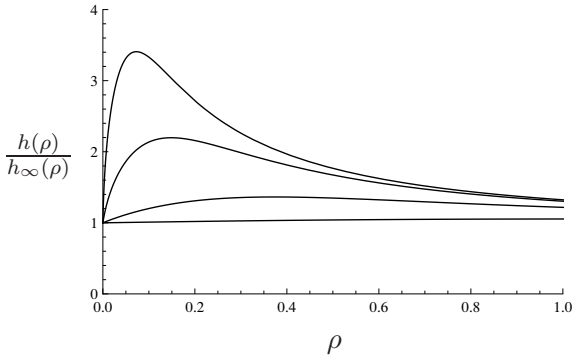

Figure 13. Convergence of the numerical solutions for singular solitons with an $\frac{a}{\rho}$ singularity to the family of approximate solutions $h_{\infty(\rho)}$ as we increase a. We plot the ratio of the two functions for various values of a and we see that it converges to 1 as we raise a. The values plotted are $a = 0.1, 0.2, 0.5, 1.5$, from top to bottom.

5.3.3 An analytic solution at large charge

While we have no analytic control of $\alpha = 1$ solutions in general, we can see from the numerical analysis that for large a the charge of the solution can be well approximated by the formula $q = \frac{a^2}{4} +$ subleading. In fact, in the limit of large a one can find an analytic form of the solution as follows: let us consider the first factor $(1 + \rho^2 h^3)$ on the l.h.s. of equation (5.2). At small value of ρ the term $\rho^2 h^3$ dominates over the 1 since by assumption $h \sim \frac{a}{\rho}$. At large values of ρ the same is true since $h \sim 1 + \frac{2q}{\rho^2}$. Hence it is not unreasonable to assume that in the limit of very large a we can make the approximation $1 + \rho^2 h^3 \approx \rho^2 h^3$ for the entire range of ρ. Then the differential equation (5.2) becomes

$$\rho\, h \left(3\, h' + \rho\, h''\right) = \left[4 - \left(2\, h + \rho\, h'\right)^2\right] \tag{5.36}$$

This equation can be solved exactly[32] and if we impose the desired behavior near $\rho = 0$ the solution is

$$h_\infty(\rho) = \sqrt{1 + \frac{a^2}{\rho^2}} \tag{5.37}$$

It is not hard to check that in the large charge limit the numerical solutions do indeed converge towards the solution (5.37) in the entire range of ρ, as shown in figure 13. The solution (5.37) goes like $\frac{a}{\rho}$ near $\rho = 0$ and like $1 + \frac{a^2}{2\rho^2}$ for large ρ. As we said this implies that the charge $q \sim \frac{a^2}{4}$. One also finds that in this limit the expectation value goes like $\langle \mathcal{O}_\phi \rangle \sim a^2$. So in the limit of large q we have

$$\langle \mathcal{O}_\phi \rangle = 4q + \ldots$$

which describes the behavior of the red curve in figure 14 for large q.

[32] The general solution of (5.36) is $h(\rho) = \sqrt{1 + \frac{c_1}{\rho^2} + \frac{c_2}{\rho^4}}$.

JHEP11(2011)035

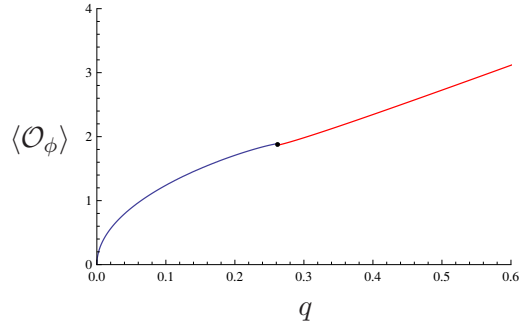

Figure 14. Expectation value $\langle \mathcal{O}_\phi \rangle$ vs charge q for the family of regular solitons (blue) and for the family of solitons with an $\frac{a}{\rho}$ singularity (red). The two curves meet at the point denoted by the black dot which corresponds to the special solution S with $\rho^{-2/3}$ behavior.

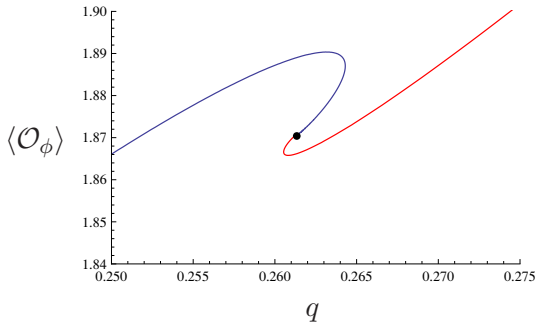

Figure 15. Detail of the previous graph around the point S where the two families meet. The blue curve is the regular soliton and the red curve is the soliton with the $\frac{a}{\rho}$ singuality.

5.4 Phase structure of 'regular' supersymmetric solutions

Let us now put everything together and describe the space of supersymmetric solutions. In figures 14, 15 we show the expectation value $\langle \mathcal{O}_\phi \rangle$ and the charge q of the family of regular solitons (blue curve) and those with an $\frac{a}{\rho}$ singularity (red curve). As we explained above the two families meet at the solution S with $\rho^{-2/3}$ behavior, which is denoted by a black dot. Near the point S the two curves develop into two intertwined spirals which are asymptotically described by equations (5.23), (5.28), (5.31), (5.34). We zoom into the point S in figures 24, 25 in appendix C.

From these figures we see that the curves are non intersecting, which means that if we fix the charge q and the expectation value $\langle \mathcal{O}_\phi \rangle$ there is at most one solution. If we consider the number of solutions as a function of the charge q leaving $\langle \mathcal{O}_\phi \rangle$ arbitrary we have the following pattern: for small enough q we have only one regular solitonic solution. As we increase q we first encounter the point q_{min} where two new solutions appear, bringing the total number of solutions to 3. Increasing q we cross a point where two more regular solutions are added and the total number of solutions becomes 5. This pattern continues as we approach the point q_c with an ever-increasing number of total solutions (at each step we add, alternatively, either two regular or two singular solutions). Notice that this number is always odd. After we cross the point q_c the pattern is reversed, we successively lose pairs of

JHEP11(2011)035

solutions until we end up with a single singular solution for $q > q_{\rm max}$. Similar statements hold if we look for solutions with given expectation $\langle \mathcal{O}_\phi \rangle$ instead of given charge. However, the fact that the curves in these figures are non-intersecting, means that if we specify both q and $\langle \mathcal{O}_\phi \rangle$ there is always at most one solitonic solution with these values.

The phase diagram we have proposed for our gravitational system is depicted in figure 2. In this diagram we have included a phase transition curve that meets the BPS line near $q = q_c \approx 0.2613$; we will now explain our rational for doing so. In this paragraph we assume that both the regular and the singular supersymmetric solutions found before, may each be obtained as a limit of non singular non extremal hairy black hole solutions. As we saw above for any given value of q we may have either one, or a larger odd number of supersymmetric configurations depending on whether q lies outside or inside the interval $(q_{\rm min}, q_{\rm max}) = (0.2605, 2643)$. It follows that there may exist more than one near supersymmetric regular hairy black hole solutions in the charge range $q \in (q_{\rm min}, q_{\rm max})$ approximately centered around q_c, on which we now focus. These configurations differ by the expectation value $\langle \mathcal{O}_\phi \rangle$ of the operator dual to the field ϕ. Let $S_R(q, \delta e)$ denote the entropy of the hairy black hole that reduces to the regular soliton with the largest value of $\langle \mathcal{O}_\phi \rangle$ when $\delta e \to 0$ (here δe denotes the energy above BPS). Let $S_S(q, \delta e)$ denote the entropy of the hairy black hole that reduces to the singular supersymmetric solutions with the smallest value of $\langle \mathcal{O}_\phi \rangle$. We suspect that

$$\begin{aligned} S_R(q, \delta e) &> S_S(q, \delta e) \quad \text{when} \quad q < q_P(\delta e) \\ S_S(q, \delta e) &> S_R(q, \delta e) \quad \text{when} \quad q > q_P(\delta e) \end{aligned} \tag{5.38}$$

for some $q_P(\delta e)$ such that $\lim_{\delta e \to 0} q_P(\delta e) \in (q_{\rm min}, q_{\rm max})$. Moreover we suspect that the entropies of the plethora of intermediate phases that appear at charges near to q_c are always smaller than either $S_S(q, \delta e)$ or $S_R(q, \delta e)$. In other words we suspect that our system undergoes the micro canonical analogue of a a single first order phase transition at $q = q_P(\delta e)$; this is the black curve we have depicted in figure 2. The phase transition curve, which originates at the BPS line, could either extend all the way to the phase transition curve between RNAdS and hairy black holes, or could terminate somewhere in the bulk of the hairy black hole phase, at a triple point analogous to the water steam system. Of course the considerations of this paragraph have been highly speculative. It would be very interesting to investigate this further.

Before we continue we would like to mention that it would be important to clarify the stability of these solutions under linearized perturbations. As mentioned in footnote 31 on general grounds one would expect regular solutions past $q_{\rm max}$ to be unstable. On the other hand our solutions are supersymmetric and from this point of view it would seem more natural to believe that they are stable. This is a confusing issue that deserves further study.

6 Thermodynamics in the micro canonical ensemble

In this section we present thermodynamical formulae for RNAdS black holes, the supersymmetric solitons, and hairy black holes, in a small charge and near extremal limit. We also demonstrate that the leading order thermodynamical formulae for hairy black holes

JHEP11(2011)035

are reproduced by modeling them by a non interacting mix of a soliton and an RNAdS black hole with $\mu = 1$.

6.1 RNAdS black hole

The basic thermodynamics for an RNAdS black hole is summarised by the following formulae

$$\begin{aligned} m \equiv \frac{M}{N^2} &= \frac{3}{4} R^2 \left[1 + R^2 + \mu^2\right] \\ q \equiv \frac{Q}{N^2} &= \frac{\mu}{2} R^2 \\ s \equiv \frac{S}{N^2} &= \pi R^3 \\ T &= \frac{1}{2\pi R} \left[1 + 2R^2 - \mu^2\right] \end{aligned} \tag{6.1}$$

were Q is the charge, M is the mass of the black hole, S is its entropy, T its temperature and μ its chemical potential. Note that

$$\mu^2 \leq (1 + 2R^2). \tag{6.2}$$

(this follows from the requirement that R is the outer rather than the inner event horizon of the black hole).

In this paper we are interested in small RNAdS black holes — i.e. black holes with $m \ll 1$ and $q \ll 1$ that are also very near extremality. The mass of RNAdS black holes at fixed charge is bounded from below by the mass of the extremal black hole of the same charge; at small q we have

$$m \geq 3\left(q + q^2 - 2q^3\right) + \mathcal{O}(q^4) \tag{6.3}$$

For every pair (m, q) that obeys this inequality, there exists a unique black hole solution. In this paper we are interested in black holes whose mass above extremality of of order $\mathcal{O}(q^3)$.[33] For this reason we define the shifted and rescaled mass variable δ^2 by

$$\delta^2 q^3 = m - 3\left(q + q^2 - 2q^3\right) \tag{6.4}$$

We are interested in $q \ll 1$ but δ of order unity. In this regime the entropy, chemical

[33] Note that the mass of an extremal black hole, at charge q, exceeds the mass of a BPS black hole at the same charge by $3q^2 - 6q^3 + \mathcal{O}(q^4)$. Consequently the deviation of the mass of our black holes from the BPS bound is given by $3q^2 + (\delta - 6)q^3$, and in particular is $\mathcal{O}(q^2)$ rather than $\mathcal{O}(q^3)$.

JHEP11(2011)035

potential and temperature of this black hole is given by[34]

$$
\begin{aligned}
s &= \pi q^{\frac{3}{2}}\left[2\sqrt{2}+\left(2\sqrt{3}\delta-6\sqrt{2}\right)q+\left(\frac{3\delta^2}{\sqrt{2}}-10\sqrt{3}\delta+33\sqrt{2}-\frac{24\sqrt{3}}{\delta}\right)q^2+O\left(q^3\right)\right]\\
\mu &= 1+\left(2-\sqrt{\frac{2}{3}}\delta\right)q+\left(\frac{\delta^2}{3}-6+\frac{4\sqrt{6}}{\delta}\right)q^2+O\left(q^3\right)\\
\pi T &= q^{\frac{1}{2}}\left[\frac{\delta}{\sqrt{3}}-\frac{\left(3\sqrt{2}\delta^3-10\sqrt{3}\delta^2+24\sqrt{3}\right)q}{6\delta}+O\left(q^2\right)\right]
\end{aligned}
\tag{6.5}
$$

Although the black holes we study are very small, their temperature is very small (it scales like $\sqrt{q}$) because we focus on the near extremal limit.[35] Moreover the black hole temperature decreases as we decrease δ, reaching zero at $\delta = 0 + \mathcal{O}(q)$.

Note also that the chemical potential μ of these black holes is unity at leading order. The first correction to this leading order result is of order $\mathcal{O}(q)$ and is positive when $\delta^2 < 6$ but negative otherwise. This already suggests that RN-AdS black holes with $\delta^2 < 6$ are unstable to super radiant decay; we will see below that this is indeed the case. As we will see below, the end point of the resultant tachyon condensation process is a hairy black hole.

Finally note that the radius of the black holes we study is $\mathcal{O}(\sqrt{q})$ so that the entropy is of order $\mathcal{O}(q^{\frac{3}{2}})$.

6.2 Supersymmetric soliton

The mass and charge of the supersymmetric soliton are given by

$$
\begin{aligned}
m &= \frac{3}{4}\left(\frac{\epsilon^2}{4}+\frac{\epsilon^4}{192}+\frac{\epsilon^6}{1920}+\frac{169\epsilon^8}{2211840}+\mathcal{O}\left(\epsilon^{10}\right)\right)\\
q &= \frac{1}{2}\left(\frac{\epsilon^2}{8}+\frac{\epsilon^4}{384}+\frac{\epsilon^6}{3840}+\frac{169\epsilon^8}{4423680}+\mathcal{O}\left(\epsilon^{10}\right)\right)
\end{aligned}
\tag{6.6}
$$

Note that

$$
\begin{aligned}
m &= 3q\\
\mu &= 1
\end{aligned}
\tag{6.7}
$$

Of course the soliton is dynamically stable as it is supersymmetric. It carries no entropy.

6.3 A non interacting mix of the black hole and soliton

In this subsection we will determine the thermodynamics of a hypothetical non interacting mixture of the small black holes and the supersymmetric solitons of the previous subsection.

[34] The reader may worry that the appearance of inverse powers of δ in (6.5) signify that black hole thermodynamics degenerate in the extremal limit; this, however, is not the case. At extremality $\delta = \delta_{ext}(q)$. The function $\delta_{ext}(q)$ starts out at $\mathcal{O}(q)$ and so is small at small charge, but does not identically vanish. Infact $\delta_{ext}(q)$ may be determined as a power expansion in q by equating the temperature in (6.5) to zero. Plugging this function into the remaining expressions in (6.5), yields nonsingular, analytic expressions as a function of q.

[35] In contrast small black holes in [14] all had a very high temperatures.

JHEP11(2011)035

Of the net mass m and charge q of the system, let mass $3q_s$ and and charge q_s lie in condensate so that the mass and charge of the black hole are given by

$$\begin{aligned} m_b &= m - 3q_s \\ q_b &= q - q_s \end{aligned} \tag{6.8}$$

The charge q_s is determined by maximising the entropy of the system, which determines the black hole chemical potential to be unity. This condition gives

$$m_b = 3q_b + 3q_b^2 \tag{6.9}$$

(this exact formula may also be verified to $\mathcal{O}(q^4)$ by setting $\delta^2 = 6$ in (6.5)) plugging (6.8) into (6.9) yields a quadratic equation for q_s. Solving this equation we find

$$\begin{aligned} q_s &= \left(q - \sqrt{\frac{m-3q}{3}} \right) \\ q_b &= \sqrt{\frac{m-3q}{3}} \end{aligned} \tag{6.10}$$

The squared radius of the black hole is given by $R_b^2 = 2q_b$. At leading order the entropy and temperature of the mixture are given by

$$\begin{aligned} s = \pi R^3 &= \pi \left(2\sqrt{\frac{m-3q}{3}} \right)^{\frac{3}{2}} \\ T &= \frac{\sqrt{2}}{\pi} \left(\frac{m-3q}{3} \right)^{\frac{1}{4}} \end{aligned} \tag{6.11}$$

As the $m-3q$ for the mixture is of order q^2, it is convenient to define a shifted and rescaled mass variable

$$q^2 \rho = \frac{4}{3}(m - 3q)$$

in terms of which

$$\begin{aligned} s &= \pi q^{\frac{3}{2}} \rho^{\frac{3}{4}} \\ T &= \sqrt{q} \frac{\rho^{\frac{1}{4}}}{\pi} \end{aligned} \tag{6.12}$$

We will see below that these results correctly reproduce the leading order thermodynamics of hairy black holes.

6.4 Hairy black hole

Once we have our solutions for hairy black holes from appendix A, the evaluation of their thermodynamic charges and potentials is a straight forward exercise. At low orders in the

JHEP11(2011)035

perturbative expansion we find

$$\begin{aligned}
\left(\frac{8G_5}{3\pi}\right) M = \frac{4M}{3N^2} = \frac{4m}{3} &= \left[2R^2 + R^4 + R^6 + \mathcal{O}(R^8)\right] \\
&+ \epsilon^2 \left[\frac{1}{4} + \frac{R^2}{4} + \left(-2\log(R) - \frac{\log(2)}{2} - \frac{3}{2}\right) R^4 + \mathcal{O}(R^6)\right] \\
&+ \epsilon^4 \left[\frac{1}{192} + \frac{29R^2}{576} + \mathcal{O}(R^4)\right] + \epsilon^6 \left[\frac{1}{1920} + \mathcal{O}(R^2)\right] + \mathcal{O}(\epsilon^8) \\
\left(\frac{4G_5}{\pi}\right) Q = \frac{2Q}{N^2} = 2q &= \left[R^2 + \frac{R^6}{2} + \mathcal{O}(R^8)\right] \\
&+ \epsilon^2 \left[\frac{1}{8} + \frac{R^2}{8} + \left(-\log(R) - \frac{\log(2)}{4} - \frac{13}{16}\right) R^4 + \mathcal{O}(R^6)\right] \\
&+ \epsilon^4 \left[\frac{1}{384} + \frac{29R^2}{1152} + \mathcal{O}(R^4)\right] + \epsilon^6 \left[\frac{1}{3840} + \mathcal{O}(R^2)\right] + \mathcal{O}(\epsilon^8) \\
\mu = &\left[1 + \frac{R^4}{2} + \mathcal{O}(R^6)\right] + \epsilon^2 \left[\frac{R^4}{6} + \mathcal{O}(R^6)\right] \\
&+ \epsilon^4 \left[\mathcal{O}(R^4)\right] + \epsilon^6 \left[\mathcal{O}(R^2)\right] + \mathcal{O}(\epsilon^8) \\
4\pi T = &\left[4R - 2R^3 + \mathcal{O}(R^5)\right] \\
&+ \epsilon^2 \left[\frac{R}{2} + R^3 \left(-12\log(R) - \log(8) - \frac{89}{12}\right) + \mathcal{O}(R^5)\right] \\
&+ \epsilon^4 \left[\frac{3R}{32} + \mathcal{O}(R^3)\right] + \epsilon^6 \left[\mathcal{O}(R)\right] + \mathcal{O}(\epsilon^8)
\end{aligned} \tag{6.13}$$

These quantities obey the second law

$$dM - 3\mu\, dQ - TdS = 0$$

where $S = \text{Entropy} = \frac{\pi^2}{2G_5} R^3 = \pi N^2 R^3$.

Upon setting $\epsilon = 0$ in (6.13) we find we find a formula for the instability curve of the RNAdS black hole. Eliminating R we find that this curve lies along the curve

$$m = 3q + 3q^2 + \mathcal{O}(q^4), \tag{6.14}$$

i.e. along the curve $\delta^2 = 6$ in the notation of subsection 6.1. Note that, along this curve, μ deviates from the value unity only at $\mathcal{O}(R^4)$.

We will now compute the entropy of the hairy black hole as a function of its mass and charge. Let us define a rescaled energy above BPS

$$\rho q^2 = \frac{4}{3}(m - 3q)$$

It may be verified that

$$\begin{aligned}
R^2 &= q\sqrt{\rho}\left[1 + \frac{q}{2}(-2 + \sqrt{\rho}) + \mathcal{O}(q^2)\right] \\
\epsilon^2 &= 8q\,(2 - \sqrt{\rho}) - \frac{8q^2}{3}(2 + \sqrt{\rho} - \rho) + \mathcal{O}\left(q^3\right)
\end{aligned} \tag{6.15}$$

JHEP11(2011)035

The temperature and chemical potential of the black hole are are given by

$$\begin{aligned} T &= \sqrt{q}\,\frac{\rho^{\frac{1}{4}}}{4\pi}\,\left[4+q(6-5\sqrt{\rho})+\mathcal{O}(q^2)\right] \\ \mu &= 1+q\frac{\rho}{2}+\mathcal{O}(q^2) \end{aligned} \tag{6.16}$$

while its entropy is given by

$$S=\pi R^3=q^{\frac{3}{2}}\pi\rho^{\frac{3}{4}}\left[1+\frac{3q}{4}\left(-2+\sqrt{\rho}\right)+q^2\frac{100-76\sqrt{\rho}+13\rho}{32}+\mathcal{O}\left(q^3\right)\right] \tag{6.17}$$

Note that (6.16) and (6.17) agree with (6.12) at leading order. It follows that, atleast for thermodynamical purposes, the hairy black hole solution may be regarded as a non interacting mix of a small RNAdS black hole and the soliton, at leading order.

7 Hairy rotating black holes

7.1 Thermodynamics of small Kerr RNAdS black holes

Large classes of explicit Kerr RNAdS black hole solutions have been presented (and their thermodynamics worked out) in [1–7]. In this subsection we focus on the special case of small near extremal black hole with self dual angular momenta and all three charges equal. Concretely, we study black holes with mass $M = N^2 m$, charge $Q = N^2 q$ and angular momentum $J = N^2 q^2 j$.[36] We will take q to be small, but allow j to be arbitrary. All our formulae below are presented in a power series expansion in q but are exact in j.

The extremality curve for the black holes we study is given by

$$m_{ext}(q,j)=3q+\left(3+\frac{j^2}{3}\right)q^2+\left(-6+\frac{10}{9}j^2-\frac{4}{81}j^4\right)q^3+\mathcal{O}(q^4) \tag{7.1}$$

In contrast the BPS bound for the theory is

$$m_{BPS}(q,j)=3q+2q^2j \tag{7.2}$$

Note that

$$m_{ext}-m_{BPS}=q^2\frac{(j-3)^2}{3}+\mathcal{O}(q^3). \tag{7.3}$$

In particular the mass of the extremal black hole always $\geq$ that of the BPS black hole. The extremal black hole is also BPS only when

$$j=3-2q+3q^2+\mathcal{O}(q^3) \tag{7.4}$$

As in previous sections, we will be interested in black holes whose energy deviates from extremality only at order $\mathcal{O}(q^3)$. To focus in on these energies, it is convenient, as in previous sections, to define a shifted and rescaled energy variable δ^2 by

$$\delta^2 q^3=m-\left[3q+\left(3+\frac{j^2}{3}\right)q^2+\left(-6+\frac{10}{9}j^2-\frac{4}{81}j^4\right)q^3\right] \tag{7.5}$$

[36] Concretely, J is the value of J_z in one of the two SU(2) factors of SO(4). As in the earlier part of this paper, the mass M is normalized to agree with the scaling dimension of dual operators, while the charge Q is normalized to be unity for a complex chiral field Z.

JHEP11(2011)035

As above we work in a power series expansion in q but our formulae are all exact in δ. With this notation, the thermodynamical potentials of small near extremal RNAdS black holes is given by

$$\begin{aligned}
\mu &= 1 + \left(2 - \frac{2}{9}j^2 - \sqrt{\frac{2}{3}}\delta\right) q + \mathcal{O}(q^2) \\
\Omega &= \frac{j}{3} - \left(\frac{10}{9}j - \frac{j\delta}{\sqrt{6}} - \frac{8j^3}{81}\right) q + \mathcal{O}(q^2) \\
\pi T &= q^{\frac{1}{2}} \left[\left(\frac{\delta}{\sqrt{3}}\right) + \mathcal{O}(q^2)\right] \\
s &= \pi q^{\frac{3}{2}} \left[2\sqrt{2} + \left(\frac{-12 + j^2 + 2\sqrt{6}\delta}{\sqrt{2}}\right) q + \mathcal{O}(q^2)\right]
\end{aligned} \tag{7.6}$$

We are particularly interested in two different two parameter surfaces in this 3 dimensional space of black holes. The first of these surfaces is the subspace of extremal black holes given by (7.2). Specializing to this surface we find

$$\begin{aligned}
\mu &= 1 + \left[2 - \frac{2j^2}{9}\right] q + \left[\frac{10}{243}j^2\left(2j^2 - 9\right) - 6\right] q^2 + \mathcal{O}(q^3) \\
\Omega &= \frac{j}{3} + \left[\frac{2}{81}j\left(45 - 4j^2\right)\right] q + \left[\frac{j}{729}\left(28j^4 - 150j^2 - 1917\right)\right] q^2 + \mathcal{O}(q^3) \\
s &= \pi q^{\frac{3}{2}} \left[2\sqrt{2} + \left(\frac{-12 + j^2}{\sqrt{2}}\right) q + \left(\frac{3j^4 + 104j^2 - 1584}{24\sqrt{2}}\right) q^2 + \mathcal{O}(q^3)\right]
\end{aligned} \tag{7.7}$$

The second surface of interest, as in previous sections, is the subspace of black holes with $\mu = 1$. We may solve for δ in terms of q in order to set $\mu = 1$; the solution is given by

$$\delta = -\sqrt{\frac{2}{27}}(j^2 - 9) + \left[\frac{j^2\left(-162 + 45j^2 + j^4\right)}{486\sqrt{6}(j^2 - 9)}\right] q + \mathcal{O}(q^4) \tag{7.8}$$

Substituting this value of δ in (7.6) we find

$$\begin{aligned}
\Omega &= \frac{j}{3} + \left(\frac{j(9 + j^2)}{81}\right) q + \left(\frac{j(-18 + j^2)}{243}\right) q^2 + \mathcal{O}(q^3) \\
\pi T &= q^{\frac{1}{2}} \left[\frac{\sqrt{2}}{9}(9 - j^2) - \left(\frac{j^2(45 + 11j^2)}{486\sqrt{2}}\right) q + \mathcal{O}(q^2)\right] \\
s &= \pi q^{\frac{3}{2}} \left[2\sqrt{2} - \left(\frac{j^2}{3\sqrt{2}}\right) q + \left(\frac{7j^4}{648\sqrt{2}}\right) q^2 + \mathcal{O}(q^3)\right]
\end{aligned} \tag{7.9}$$

Notice that the $\mu = 1$ surface intersects the extremality surface along the line of supersymmetric black holes. Indeed, plugging the relation (7.4) into (7.7) we find

$$\begin{aligned}
\mu &= 1 + \mathcal{O}(q^3) \\
\Omega &= 1 + \mathcal{O}(q^2)
\end{aligned} \tag{7.10}$$

In fact it may be shown that the equation $\mu = \Omega = 1$ is exact for supersymmetric black holes.[37]

[37] We thank Seok Kim for explaining this to us.

JHEP11(2011)035

7.2 Hairy rotating black holes as a non interacting mix

We have seen in the previous section that the thermodynamics of Hairy AdS black holes is very simply reproduced, at leading order, by a simple physical picture of the black hole as a non interacting mix of the RNAdS black hole and the soliton. In this section we will simply assume the same is true of charged rotating hairy black holes. In other words we assume that there exist charged rotating black holes whose thermodynamics, at leading order, is reproduced by an arbitrarily weakly interacting mix of the spherically symmetric soliton of previous sections,[38] and the small spinning RNAdS Kerr black hole. As in the previous section, the condition for thermodynamical equilibrium of this mix is simply the requirement that the Kerr RNAdS black hole, that participates in this mix, has $\mu = 1$.

The charge, angular momentum and energy of such an equilibrated mix is given by

$$\begin{aligned} q &= q_b + q_s \\ jq^2 &= j_b q_b^2 \\ m &= \left[3q_b + \frac{1}{3}(j_b^2+9)q_b^2 + \mathcal{O}(q_b^3)\right] + 3q_s \end{aligned} \tag{7.11}$$

The three equations (7.11) may be used to solve for q_b, q_s and j_b in terms of q, j and m. At leading order we find

$$\begin{aligned} q_b &= \left[\frac{(m-3q)+\sqrt{(m-3q)^2-4j^2q^4}}{6}\right]^{\frac{1}{2}} \\ j_b &= \frac{6jq^2}{(m-3q)+\sqrt{(m-3q)^2-4j^2q^4}} \\ q_s &= q - \left[\frac{(m-3q)+\sqrt{(m-3q)^2-4j^2q^4}}{6}\right]^{\frac{1}{2}} \end{aligned} \tag{7.12}$$

It then follows that the entropy, temperature and angular chemical potential of the mix, are given at leading order by

$$\begin{aligned} s &= 2\sqrt{2}\pi\left[\frac{(m-3q)+\sqrt{(m-3q)^2-4j^2q^4}}{6}\right]^{\frac{3}{4}} \\ \pi T &= \sqrt{2}\left(\frac{(m-3q)+\sqrt{(m-3q)^2-4j^2q^4}}{6}\right)^{\frac{1}{4}}\left(1-\frac{4j^2q^4}{\left((m-3q)+\sqrt{(m-3q)^2-4j^2q^4}\right)^2}\right) \\ \Omega &= \frac{j_b}{3} \end{aligned} \tag{7.13}$$

[38] It should also be possible to study rotating black holes in equilibrium with solitons made out of the condensates of other supergravity modes, e.g. modes of the graviton. At small total angular momentum, however, the only modes of the chiral ring satisfy the thermodynamical requirement of non interacting equilibrium. This changes at angular momenta exceeding unity at which point equilibrium between spinning black holes and the solitons of this paper becomes impossible (see below), but rotating black holes could presumably equilibrate with other solitons. We thank H. Reall for a discussion on this point, and leave the discussion of black holes immersed in other solitonic backgrounds to future work.

JHEP11(2011)035

Note that the hairy black holes of this subsection exist only for $j < 3$ (this follows because $j_b \geq j$ whenever $q_s > 0$ (as we have assumed), but black holes with $j_b > 3$ have negative temperature and so a naked singularity). When this condition is satisfied, they exist provided

$$3q + 2jq^2 \leq m \leq 3q + \frac{1}{3}(j^2+9)q^2 - \frac{2}{81}j^2(j^2+9)q^3 \tag{7.14}$$

The range of this existence interval shrinks to zero as j approaches 3.

At the upper end of this mass range we find, from (7.12), that $q_b = q$, $j_b = j$ and $q_s = 0$; i.e. the hairy black hole reduces to a pure RNAdS black hole. At the lower end of this range (i.e. when the system charges satisfy the BPS bound $m - 3q = 2jq^2$) on the other hand (7.15) reduces to

$$\begin{aligned} q_b &= q\left[\frac{j}{3}\right]^{\frac{1}{2}} \\ j_b &= 3 \\ q_s &= q\left(1 - \sqrt{\frac{j}{3}}\right) \end{aligned} \tag{7.15}$$

At this lower end, then, the temperature of the hairy black vanishes. At this end the hairy black hole is neither pure soliton (unless $j = 0$) or pure black hole (unless $j = 3$; at which value the upper and lower end of (7.14) coincide) but a mix of soliton and black hole. The special feature of this mix is that $j_b = 3$, so that the participating black hole is supersymmetric. At the lower edge, then, the system is a weakly interacting mix of a supersymmetric black hole and the supersymmetric condensate, and is itself supersymmetric. This is of course intuitive. An extremal hairy black hole is given by a non interacting mix of an extremal Kerr RNAdS black hole with $\mu = 1$ and a soliton. But, as we have seen above, extremal Kerr RNAdS black holes are BPS at $\mu = 1$. It follows that (within the approximations of this subsection), that the extremal hairy black hole is also BPS.

Note that the approximations of this subsection predict a two parameter family of BPS hairy black holes (the entire lower edge of (7.14)) in comparison with the one parameter set of BPS Kerr RNAdS black holes. These black holes constitute the lower end of the mass range (7.14).

To end this section we should emphasize that all the formulae of this section are predicated on the assumption that hairy black hole thermodynamics may be reproduced, at leading order, by a non interacting mixture of a Kerr RNAdS black hole and a scalar condensate. While we have checked by explicit calculation that this guess is true in the absence of rotation, we have not yet performed any such check for rotating black holes. The reader should, consequently, regard the formulae of this section as conjectural. As we have remarked in the introduction, it may well prove technically possible to verify (or diversify) the predictions of this subsection by an explicit perturbative calculation of the sort presented earlier in this paper. We leave this effort for future work.

JHEP11(2011)035

8 Discussion

In this paper we have studied charged black holes in global AdS spaces. We have focused mainly on spherically symmetric black holes with equal diagonal SO(6) charges. At small values of the charge we have demonstrated that the spectrum of AdS hairy black holes extends all the way down to the BPS bound. We have also conjectured that this result applies at all values of the charge. The evidence for this last conjecture is not yet overwhelming, it would certainly be worthwhile to gather other evidence (e.g. from numerical solutions of the relevant differential equations) to support or refute this claim, as also to verify the precise nature of the large charge singular supersymmetric solutions proposed in subsection 5.3.3.

The special singular solution S, discussed in section 5, appears to play a very special role in the space of supersymmetric solutions of the theory. It would be interesting to study the near singularity geometry of this solution in more detail; in particular it would be very interesting to determine the 10 dimensional lift of this solution, as well those of the $\alpha = 1$ singular solutions of section 5. It is conceivable that these singular five dimensional solutions have a regular ten dimensional lift. If this is not the case the ten dimensional perspective should at least yield valuable insight into the nature of the singularities in these solutions. It may also be worthwhile to re investigate the nature of $\alpha = 2$ supersymmetric solutions from the ten dimensional viewpoint.

Let us momentarily turn to the consideration of black branes in asymptotically Poincare AdS spaces. These solutions may be obtained from the large charge limit of the black hole solutions studied in this paper. RNAdS black branes solutions exist at all values of $\rho_e \geq c_e \rho_q^{\frac{4}{3}}$ with $c_e = \frac{9}{2}\pi^{2/3}$. These solutions are presumably unstable to the condensation of the ϕ field for energy densities $\rho_e \leq c_s \rho_q^{\frac{4}{3}}$ for some $c_s > c_e$. If hairy black branes at a given charge density have a lower bound on their energy density, the equation for this lower bound must also take the form $\rho_e \geq c_m \rho_q^{\frac{4}{3}}$ with $c_m < c_e$. It is clearly of interest to know the value of c_m. Our conjecture that hairy black holes descend down to their BPS bound even at large charge amounts to the prediction that $c_m = 0$, i.e. there is no lower bound for the mass density of hairy black branes, at any fixed finite charge density. This phenomenon is not without known precedent; as we explain in appendix B, a similar result is true of one charge (rather than 3 equal charge, as studied in this paper) RNAdS black branes.

On a related note, the recent paper [36] has presented an analytic determination of the constant c_s (and the hairy black brane solution in the neighborhood of this critical density) in a system with some similarities to the one studied in this paper. In particular the scalar field in [36] has the same value of the mass as in the current work, but carries infinite charge (this is the so called the probe approximation that ignores the backreaction of gauge dynamics on the metric). It would be interesting to investigate whether the results of [36] can be generalized to the study of our Lagrangian (1.2).

It would be of interest to extend the results of this paper to the case of charged black holes with three unequal SO(6) charges, and particularly to study special limits in which one or two of these charges are turned off. In particular, in the special case where only

JHEP11(2011)035

one SO(6) charge is nonzero, ordinary RNAdS black holes extend all the way down to the BPS bound, so there is no pressing reason for these solutions to exhibit a superradiant instability, or for one charge hairy black brane solutions to exist. This question deserves further investigation.

It it would be fascinating to verify the correctness or otherwise of the tentative predictions of section 7 for the spectrum of small rotating black holes. In particular, if new physically acceptable supersymmetric hairy black holes really do exist, it would be fascinating to determine them and to analyse their properties.

As we have mentioned in the introduction, it is possible that the black holes we have constructed suffer from a superradiant instability towards the emission of the gravity modes dual to $TrX^n + TrY^n + TrZ^n$. It should in principle be straightforward (though perhaps tedious in practice) to check whether or not this is the case, by computing the imaginary part of the relevant quasinormal modes, along the lines of appendix A of [14].

In this paper we have focused only on a very particular kind of hairy black hole; one whose condensate is the zero mode of a scalar field in AdS_5 space. It is likely that there exist many different such hairy solutions with various different gravitational field condensates. In the current paper we have likely illuminated only a very small part of an intricate and fascinating structure of hairy black hole solutions in $AdS_5 \times S^5$. It would be fascinating to more fully uncover the structure of new black hole solutions in $AdS_5 \times S^5$, and perhaps most importantly, to understand their properties directly from the dual Yang Mills point of view.

Acknowledgments

We would like to thank J. Bhattacharya, J. de Boer, R. Loganayagam, M. Shigemori, A. Strominger, N. Suryanarayana and S. Trivedi for useful discussions. We would like especially to thank S. Kim for collaboration over the initial stages of this project, and several very useful discussions over every stage of this project. We would also like to especially thank V. Hubeny and M. Rangamani for suggesting we look for oscillatory behavior of the supersymmetric solutions near the critical charge. We would also like to thank J. Bhattacharya, C. Herzog, V. Hubeny, P. Mitra, M. Rangamani, H. Reall for useful comments on a draft version of this manuscript. SM would like to thank the Weizmann Institute and the organizers of the SERC school at Punjab University, Chandigarh and the Institute of Mathematical Sciences, Chennai, for hospitality while this work was being completed. The work of SM was supported in part by a Swarnajayanti Fellowship. S.B. and S.M. would also like to acknowledge their debt to the steady and generous support of the people of India for research in basic science.

A Results for the perturbative expansion of hairy black holes

A.1 Far field solution

Scalar field:

$$\phi^{\text{out}}_{(1,0)}(r) = \frac{1}{1+r^2}$$

JHEP11(2011)035

$$
\begin{aligned}
\phi^{\rm out}_{(1,2)}(r) =& \frac{2\left[\left(r^2+1\right)\log\left(1+\frac{1}{r^2}\right)-1\right]}{\left(r^2+1\right)^2}\\
\phi^{\rm out}_{(1,4)}(r) =& \frac{8r^4+14r^2+2}{r^2\left(r^2+1\right)^3}+\frac{2\left(r^2+1\right)\log^2\left(1+\frac{1}{r^2}\right)-\left(9r^2+13\right)\log\left(1+\frac{1}{r^2}\right)}{\left(r^2+1\right)^2}\\
\phi^{\rm out}_{(3,0)}(r) =& \frac{1}{8(1+r^2)^3}\\
\phi^{\rm out}_{(3,2)}(r) =& \frac{r^2+6\left(r^2+1\right)\log\left(1+\frac{1}{r^2}\right)-5}{8\left(r^2+1\right)^4}\\
\phi^{\rm out}_{(5,0)}(r) =& \frac{6r^4+4r^2+55}{2304\left(r^2+1\right)^5}\\
\phi^{\rm out}_{(5,2)}(r) =& \frac{1}{6912\left(r^2+1\right)^6}\Bigg[-1091+923r^2+562r^4+282r^6+24r^8\\
&+6\left(r^2+1\right)\left(4r^8+16r^6-6r^4-4r^2-271\right)\log\left(\frac{r^2}{r^2+1}\right)\Bigg]
\end{aligned}
\tag{A.1}
$$

Metric and gauge field:

$$
\begin{aligned}
f^{\rm out}_{(2,0)}(r) =& -\frac{1}{4(1+r^2)}, \qquad g^{\rm out}_{(2,0)}(r)=0, \qquad A^{\rm out}_{(2,0)}(r)=-\frac{1}{8(1+r^2)}\\
f^{\rm out}_{(2,2)}(r) =& -\frac{\log\left(1+\frac{1}{r^2}\right)}{r^2+1}-\frac{r^4-3r^2-2}{4r^2\left(r^2+1\right)^2}\\
g^{\rm out}_{(2,2)}(r) =& \frac{1}{4\left(r^2+1\right)^3}\\
A^{\rm out}_{(2,2)}(r) =& -\frac{\log\left(1+\frac{1}{r^2}\right)}{2\left(r^2+1\right)}+\frac{-r^4+2r^2+1}{8r^2\left(r^2+1\right)^2}\\
f^{\rm out}_{(4,0)}(r) =& -\frac{r^4}{192\left(1+r^2\right)^3}, \qquad g_{(4,0)}(r)=\frac{r^4}{192\left(1+r^2\right)^3}\\
A^{\rm out}_{(4,0)}(r) =& -\frac{3+3r^2+r^4}{384\left(1+r^2\right)^3}\\
f^{\rm out}_{(4,2)}(r) =& -\frac{29r^6+71r^4+96r^2-24\left(r^6+r^4\right)\log\left(\frac{r^2}{r^2+1}\right)+36}{576\left(r^2+1\right)^4}\\
g^{\rm out}_{(4,2)}(r) =& \frac{29r^6+71r^4+108r^2+24\left(r^6+r^4\right)\log\left(1+\frac{1}{r^2}\right)+36}{576\left(r^2+1\right)^6}\\
A^{\rm out}_{(4,2)}(r) =& -\frac{-9+90r^4+92r^6+29r^8}{1152r^2\left(1+r^2\right)^4}-\frac{r^4+3r^2+3}{48\left(1+r^2\right)^3}\log\left(\frac{r^2}{r^2+1}\right)
\end{aligned}
\tag{A.2}
$$

A.2 Intermediate solution

$$
\phi^{\rm mid}_{(1,0)}(y)=1
$$

$$
\phi^{\rm mid}_{(1,2)}(y) = -y^2-4\log(R)-2\log\left(y^2-1\right)-2
$$

JHEP11(2011)035

$$
\begin{aligned}
\phi^{\rm mid}_{(1,4)}(y) &= 8\log^2(R) + \left(4y^2 + 8\log\left(y^2-1\right) + \frac{4}{y^2-1} + 26\right)\log(R) + \frac{y^6+5y^4+4y^2}{y^2-1} \\
&\quad + \frac{\log\left(y^2-1\right)\left(2y^4+11y^2+2\left(y^2-1\right)\log\left(y^2-1\right)-15\right)+\log(4)-16}{y^2-1} \\
\phi^{\rm mid}_{(3,0)}(y) &= \frac{1}{8} \\
\phi^{\rm mid}_{(3,2)}(y) &= \frac{1}{8}\left(-3y^2 - 12\log(R) - 6\log\left(y^2-1\right) - 5\right) \\
\phi^{\rm mid}_{(5,0)}(y) &= \frac{55}{2304} \\
\phi^{\rm mid}_{(5,2)}(y) &= \frac{-813y^2 - 3252\log(R) - 1626\log\left(y^2-1\right) - 1091}{6912}
\end{aligned}
\tag{A.3}
$$

Metric and gauge field:

$$
\begin{aligned}
f^{\rm mid}_{(2,0)}(y) &= -\frac{(y^2-1)^2}{4y^4} \\
g^{\rm mid}_{(2,0)}(y) &= 0 \\
A^{\rm mid}_{(2,0)}(y) &= -\frac{y^2-1}{8y^2} \\
f^{\rm mid}_{(2,2)}(y) &= \frac{\left(y^2-1\right)\left[y^4+\left(8y^2-4\right)\log(R)+\left(4y^2-6\right)\log\left(y^2-1\right)+\log(4)-1\right]}{4y^4} \\
g^{\rm mid}_{(2,2)}(y) &= \frac{y^4\left[y^2-4\log(R)+2\log\left(y^2-1\right)-\log(4)-5\right]}{4\left(y^2-1\right)^3} \\
A^{\rm mid}_{(2,2)}(y) &= \frac{y^4+\left(8y^2-4\right)\log(R)+\left(4y^2-6\right)\log\left(y^2-1\right)+\log(4)-1}{8y^2} \\
f^{\rm mid}_{(4,0)}(y) &= 0 \\
g^{\rm mid}_{(4,0)}(y) &= 0 \\
A^{\rm mid}_{(4,0)}(y) &= -\frac{1}{128}\left(1-\frac{1}{y^2}\right) \\
f^{\rm mid}_{(4,2)}(y) &= -\frac{\left(y^2-3\right)\left(y^2-1\right)}{16y^4} \\
g^{\rm mid}_{(4,2)}(y) &= \frac{y^4\left(y^2-4\log(R)+2\log\left(y^2-1\right)-\log(4)-7\right)}{16\left(y^2-1\right)^3} \\
A^{\rm mid}_{(4,2)}(y) &= \frac{y^4-2y^2+\left(8y^2-4\right)\log(R)+2\left(2y^2-3\right)\log\left(y^2-1\right)+\log(4)+5}{64y^2}
\end{aligned}
\tag{A.4}
$$

A.3 Near field solution

Scalar field:

$$
\begin{aligned}
\phi^{\rm in}_{(1,0)}(z) &= 1 \\
\phi^{\rm in}_{(1,2)}(z) &= -8\log(R) - \frac{1}{2}\log(z+1)(\log(z+1)+4) - {\rm Li}_2(-z) - 2\log(2) - \frac{\pi^2}{6} - 3 \\
\phi^{\rm in}_{(3,0)}(z) &= \frac{1}{8}
\end{aligned}
$$

JHEP11(2011)035

$$\begin{aligned}
\phi^{\rm in}_{(3,2)}(z) &= \frac{2(4+3\log(2))z+\pi^2(z+1)+6\log(2)+12}{8(z+1)} \\
&+\frac{3}{8}(\log(z)+i\pi-2)\log(z+1)-3\log(R)+\frac{3}{8}{\rm Li}_2(z+1) \\
&-\frac{(3z(z+1)+2)\log^2(z+1)}{16z(z+1)} \\
\phi^{\rm in}_{(5,0)}(z) &= \frac{55}{2304}
\end{aligned} \tag{A.5}$$

Metric and gauge field:

$$\begin{aligned}
f^{\rm in}_{(2,4)}(z) &= -z^2-\frac{1}{2}(2z+1)\log(z+1) \\
g^{\rm in}_{(2,-2)}(z) &= \frac{(2z+1)\log(z+1)-4z}{32z^2(z+1)^2} \\
A^{\rm in}_{(2,2)}(z) &= \frac{1}{4}(-z-\log(z+1)) \\
f^{\rm in}_{(4,4)}(z) &= \frac{z(4z+2)+\log(z+1)((z+1)\log(z+1)-1)}{16(z+1)} \\
g^{\rm in}_{(4,-2)}(z) &= \frac{(5-12z)z^2+(4(z-2)z-3)\log(z+1)z+(3z(z+1)+1)\log^2(z+1)}{256z^3(z+1)^3} \\
A^{\rm in}_{(4,2)}(z) &= -\frac{z(z+2\log(z+1)-3)}{64(z+1)}
\end{aligned} \tag{A.6}$$

B Supersymmetric solitons in $AdS_5 \times S^5$ and the planar limit

B.1 One-charge solitons

In this paper we studied supersymmetric configurations in $AdS_5 \times S^5$ by considering a truncation of $\mathcal{N}=8$ supergravity where all 3 charges corresponding to the three orthogonal planes of SO(6) are taken to be equal. The spherically symmetric supersymmetric solutions of this truncation are 1/8 BPS from the ten dimensional point of view. It is instructive to briefly review solutions of $\mathcal{N}=8$ supergravity where we turn on only one of these charges. Spherically symmetric supersymmetric configurations of this type are 1/2 BPS and belong to the LLM family [37]. We look for static, spherically symmetric 1/2 BPS solitonic solutions with the topology of $AdS_5 \times S^5$ (so that in the LLM language they have the topology of a disk). These can be studied in a truncation of $\mathcal{N}=8$ to $\mathrm{U}(1)^3$ coupled to 3 hypermultiplets, by turning on only one of the U(1) charges and can be expressed in the language of [15, 16] as[39]

$$\begin{aligned}
ds^2 &= -\frac{1+\rho^2 h}{h^{-2/3}}dt^2+\frac{h^{1/3}}{1+\rho^2 h}d\rho^2+h^{1/3}\rho^2 d\Omega_3^2 \\
A_1 = A_2 = 0, &\qquad A_3 = h^{-1}dt, \qquad X_1 = X_2 = h^{1/3}, \qquad X_3 = h^{-2/3} \\
\phi_1 = \phi_2 = 0, &\qquad \phi_3 = 2\sqrt{(h+\rho h'/2)^2-1}
\end{aligned} \tag{B.1}$$

[39] We use somewhat different notation with $r_{there} = \rho_{here}$, $(H_1)_{there} = (H_2)_{there} = 1$, $(H_3)_{there} = h_{here}$, $(A_i)_{there} = -(A_i)_{here}$, $2\sinh\phi_{i,there} = \phi_{i,here}$.

JHEP11(2011)035

where A_i are the 3 U(1) gauge fields, X_i the scalars in the vector multiplets constrained to satisfy $X_1X_2X_3 = 1$ and ϕ_i scalars in the hypermultiplets. This is a solution if $h(\rho)$ satisfies the equation

$$(1+\rho^2 h)(3h' + \rho h'') = \rho[4 - (2h + \rho h')^2] \tag{B.2}$$

Notice the different powers of h in the metric (B.1) relative to the 3-equal-charge case (5.1). Also, unlike equation (5.2), now (B.2) can be solved analytically and we find the following set of smooth solutions [15, 16]

$$h(\rho) = \sqrt{1 + 2\frac{1+2q}{\rho^2} + \frac{1}{\rho^4}} - \frac{1}{\rho^2}$$

The parameter q corresponds to the charge. In contrast to the 3-charge case which was studied in the rest of the paper, now q is unbounded from above i.e. there is no maximum charge of smooth spherically symmetric 1/2 BPS solitons similar to (5.22).

In particular we can try to recover a spacetime which is asymptotically the Poincare Patch by taking the large charge limit. We consider the following scaling

$$\begin{gathered} t = k^{-1}\,\tau, \quad \rho = k\,u, \quad \Omega_i = k^{-1}\,x_i, \quad q = q_0\,k^2 \\ \tau\,, u\,, x_i\,, q_0 \;= \text{const} \qquad , \qquad k \to \infty \end{gathered} \tag{B.3}$$

Then we find the following solution

$$\begin{gathered} ds^2 = -u^2\left(1+\frac{4q_0}{u^2}\right)^{1/6} d\tau^2 + \frac{1}{u^2\left(1+\frac{4q_0}{u^2}\right)^{1/3}} du^2 + u^2\left(1+\frac{4q_0}{u^2}\right)^{1/6} dx_i^2 \\ A_1 = A_2 = A_3 = 0\,, \qquad X_1 = X_2 = \left(1+\frac{4q_0}{u^2}\right)^{1/6}, \qquad X_3 = \left(1+\frac{4q_0}{u^2}\right)^{-1/3} \\ \phi_1 = \phi_2 = 0, \qquad \phi_3 = \frac{4q_0}{u\sqrt{4q_0+u^2}} \end{gathered} \tag{B.4}$$

which is asymptotically the Poincare Patch and has scalar fields turned on in the interior.

Let us finally consider the non-extremal one-charge RNAdS black branes. We start with a non-extremal one-charge RNAdS black hole in global AdS. We have the following solution

$$\begin{gathered} ds^2 = -H^{-2/3} f dt^2 + H^{1/3}(f^{-1}d\rho^2 + \rho^2 d\Omega_3^2) \\ A_1 = A_2 = 0, \quad A_3 = \frac{\sqrt{b(\mu+b)}}{\rho^2+b}dt\,, \qquad X^1 = X^2 = H^{1/3}, \qquad X^3 = H^{-2/3} \\ \phi_1 = \phi_2 = \phi_3 = 0 \\ H = 1 + \frac{b}{\rho^2}, \qquad f = 1 - \frac{\mu}{\rho^2} + \rho^2 H \end{gathered} \tag{B.5}$$

JHEP11(2011)035

whose charge is $q = \sqrt{b(\mu+b)}$ and mass $m = \frac{3}{2}\mu + q$. The black hole is extremal (and singular, i.e. the superstar) when $\mu = 0$. We now take the scaling

$$\begin{gathered} t = k^{-1}\,\tau, \quad \rho = k\,u, \quad \Omega_i = k^{-1}\,x_i, \quad b = b'\,k^2, \quad \mu = \mu' k^4 \\ \tau\,, u\,, x_i,\, b',\, \mu' = \text{const} \qquad , \qquad k \to \infty \end{gathered} \tag{B.6}$$

Then we find the following non-extremal charged brane solution

$$\begin{gathered} ds^2 = -\left(1+\frac{b'}{u^2}\right)^{-2/3}\left(u^2+b'-\frac{\mu'}{u^2}\right)d\tau^2+\left(1+\frac{b'}{u^2}\right)^{1/3}\left(\left(u^2+b'-\frac{\mu'}{u^2}\right)-1du^2+u^2dx_i^2\right) \\ A_1 = A_2 = 0, \quad A_3 = \frac{\sqrt{b'\mu'}}{u^2+b'^2}dt\,, \qquad X^1 = X^2 = \left(1+\frac{b'}{u^2}\right)^{1/3}, \qquad X^3 = \left(1+\frac{b'}{u^2}\right)^{-2/3}, \\ \phi_1 = \phi_2 = \phi_3 = 0 \end{gathered} \tag{B.7}$$

The energy density and charge density of this solution is (up to numerical factors of order one)

$$\rho_e \approx \mu', \qquad \rho_q \approx \sqrt{b'\mu'}$$

We notice that

$$\frac{\rho_e}{\rho_q^{4/3}} \approx (\mu')^{1/3}(b')^{-2/3}$$

we notice that by taking μ' small enough we can make this ratio as small as we like. Hence for any finite charge density, the energy density of one-charge RNAdS black branes can be made arbitrarily small i.e. the constant c_e mentioned in section 8 is $c_e = 0$ for the one-charge case.

B.2 Three-charge solitons

A similar scaling can be performed for the 1/8 BPS (3-equal charge) soliton. For this one takes the following scaling of solution of the $\frac{a}{\rho}$ form

$$\begin{gathered} t = k^{-1}\,\tau, \quad \rho = k\,u, \quad \Omega_i = k^{-1}\,x_i, \quad a = 2\sqrt{q_0}\,k \\ \tau\,, u\,, x_i\,, q_0 \;= \text{const} \qquad , \qquad k \to \infty \end{gathered} \tag{B.8}$$

For large a the solution (5.37) becomes a good approximation and from (5.1) we end up with the following hairy, asymptotically Poincare Patch solution of (2.4)

$$\begin{gathered} ds^2 = -u^2\left(1+\frac{4q_0}{u^2}\right)^{1/2}d\tau^2 + \frac{1}{u^2\left(1+\frac{4q_0}{u^2}\right)}du^2 + u^2\left(1+\frac{4q_0}{u^2}\right)^{1/2}dx_i^2 \\ A = 0 \qquad , \qquad \phi = \frac{4q_0}{u\sqrt{4q_0+u^2}} \end{gathered} \tag{B.9}$$

It would be interesting to explore whether the solution (B.9) has any relation to hairy black branes near the BPS limit.

JHEP11(2011)035

C Some numerical results

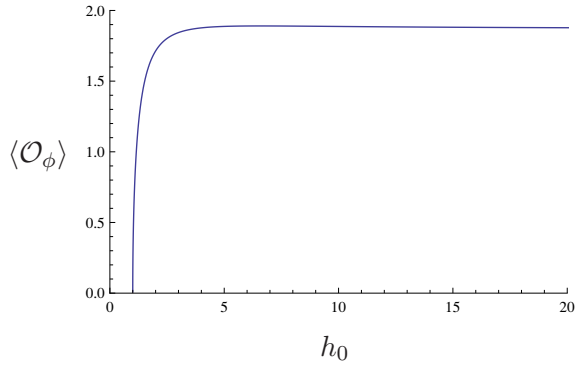

Figure 16. Expectation value $\langle \mathcal{O}_\phi \rangle$ of the operator dual to the field ϕ as a function of the value of h_0 at $r = 0$.

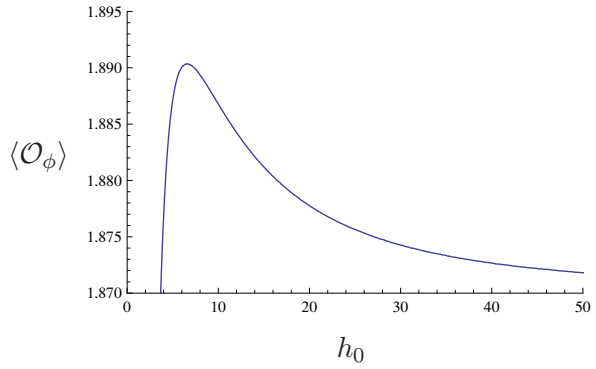

Figure 17. Detail of the previous graph with different scales on the axes, where we can see the local maximum.

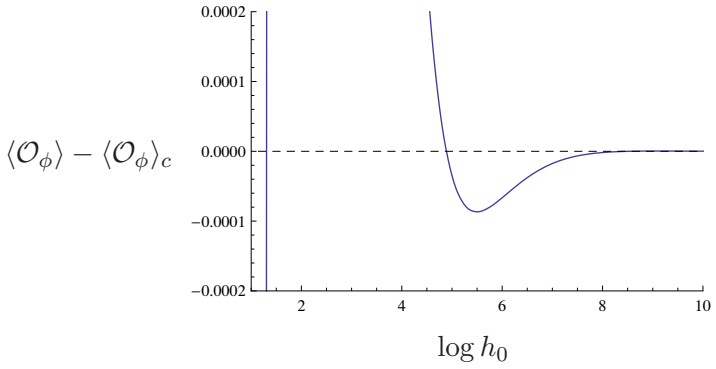

Figure 18. Magnification of the previous plot. We see the next oscillation around $\langle \mathcal{O}_\phi \rangle$.

JHEP11(2011)035

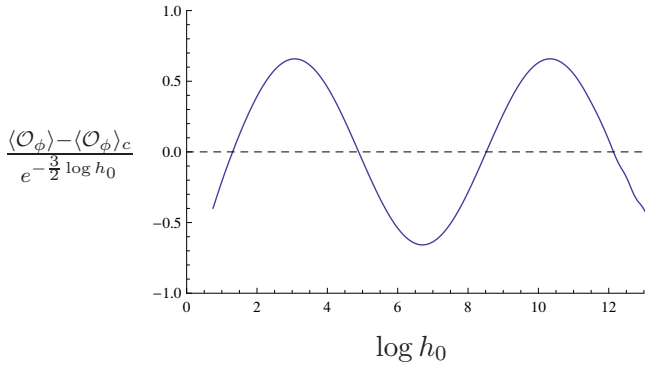

Figure 19. The damped oscillations of $\langle\mathcal{O}_\phi\rangle$ around the critical value $\langle\mathcal{O}_\phi\rangle_c$ for large h_0.

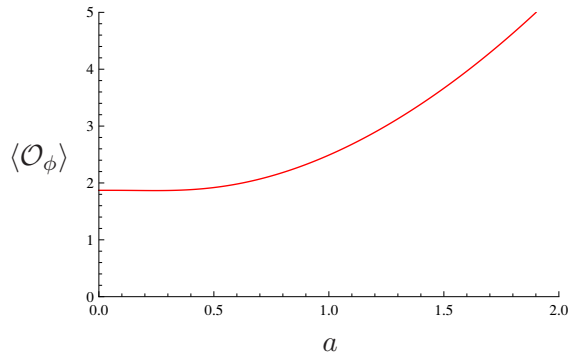

Figure 20. Expectation value $\langle\mathcal{O}_\phi\rangle$ for spherically symmetric supersymmetric solitons with a singularity of the form $\frac{a}{\rho}$ at $\rho = 0$.

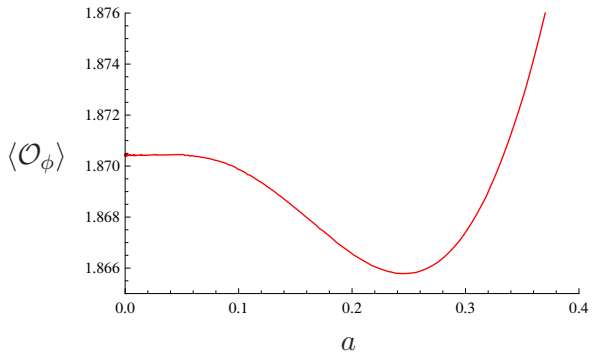

Figure 21. Detail of the previous graph with different scales on the axes, where we can see the minimum of $\langle\mathcal{O}_\phi\rangle$.

JHEP11(2011)035

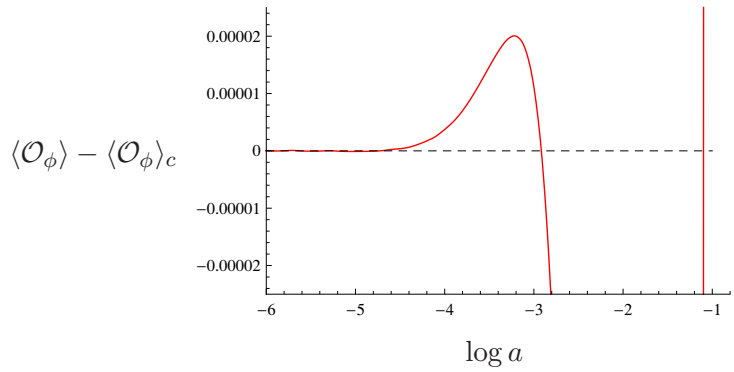

Figure 22. Magnification of the previous graph. We wee the next oscillation around $\langle\mathcal{O}_\phi\rangle$.

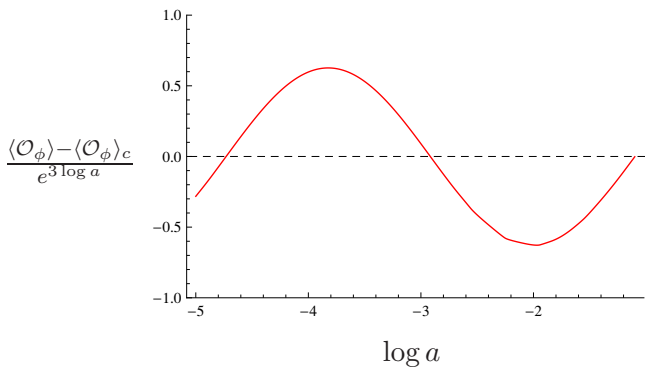

Figure 23. The damped oscillations of $\langle\mathcal{O}_\phi\rangle$ around the critical value $\langle\mathcal{O}_\phi\rangle_c$ for small a.

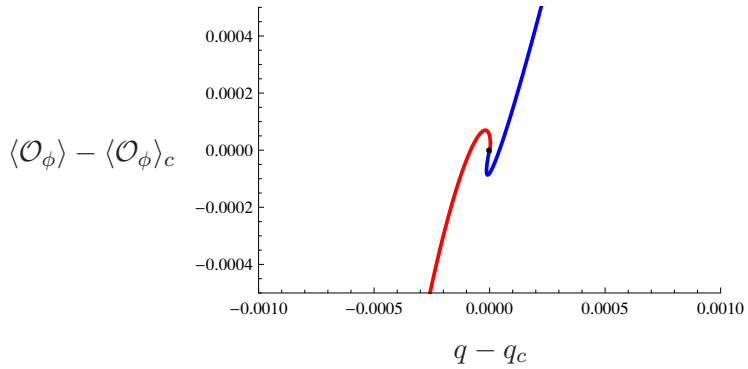

Figure 24. Zooming in around the point S. The blue curve is the regular soliton and the red curve is the soliton with the $\frac{a}{\rho}$ singuality.

JHEP11(2011)035

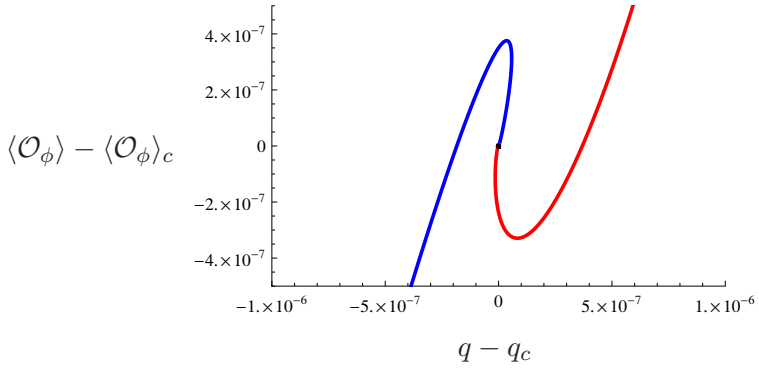

Figure 25. Further magnification around the point S. The blue curve is the regular soliton and the red curve is the soliton with the $\frac{a}{\rho}$ singuality.

References

[1] G. Gibbons, H. Lü, D.N. Page and C. Pope, *The general Kerr-de Sitter metrics in all dimensions*, *J. Geom. Phys.* **53** (2005) 49 [hep-th/0404008] [INSPIRE].

[2] G. Gibbons, M. Perry and C. Pope, *The first law of thermodynamics for Kerr-Anti-de Sitter black holes*, *Class. Quant. Grav.* **22** (2005) 1503 [hep-th/0408217] [INSPIRE].

[3] M. Cvetič, H. Lü and C. Pope, *Charged rotating black holes in five dimensional* $\mathrm{U}(1)^3$ *gauged* $N = 2$ *supergravity*, *Phys. Rev.* **D 70** (2004) 081502 [hep-th/0407058] [INSPIRE].

[4] Z.-W. Chong, M. Cvetič, H. Lü and C. Pope, *General non-extremal rotating black holes in minimal five-dimensional gauged supergravity*, *Phys. Rev. Lett.* **95** (2005) 161301 [hep-th/0506029] [INSPIRE].

[5] Z. Chong, M. Cvetič, H. Lü and C. Pope, *Five-dimensional gauged supergravity black holes with independent rotation parameters*, *Phys. Rev.* **D 72** (2005) 041901 [hep-th/0505112] [INSPIRE].

[6] Z. Chong, M. Cvetič, H. Lü and C. Pope, *Non-extremal rotating black holes in five-dimensional gauged supergravity*, *Phys. Lett.* **B 644** (2007) 192 [hep-th/0606213] [INSPIRE].

[7] M. Cvetič, G. Gibbons, H. Lü and C. Pope, *Rotating black holes in gauged supergravities: thermodynamics, supersymmetric limits, topological solitons and time machines*, hep-th/0504080 [INSPIRE].

[8] S. Sachdev, *Condensed matter and AdS/CFT*, arXiv:1002.2947 [INSPIRE].

[9] G.T. Horowitz, *Introduction to holographic superconductors*, arXiv:1002.1722 [INSPIRE].

[10] S.A. Hartnoll, *Quantum critical dynamics from black holes*, arXiv:0909.3553 [INSPIRE].

[11] S.A. Hartnoll, *Lectures on holographic methods for condensed matter physics*, *Class. Quant. Grav.* **26** (2009) 224002 [arXiv:0903.3246] [INSPIRE].

JHEP11(2011)035

[12] C.P. Herzog, *Lectures on holographic superfluidity and superconductivity*, *J. Phys.* **A 42** (2009) 343001 [arXiv:0904.1975] [INSPIRE].

[13] S.S. Gubser, *Breaking an Abelian gauge symmetry near a black hole horizon*, *Phys. Rev.* **D 78** (2008) 065034 [arXiv:0801.2977] [INSPIRE].

[14] P. Basu, J. Bhattacharya, S. Bhattacharyya, R. Loganayagam, S. Minwalla, et al., *Small hairy black holes in global AdS spacetime*, *JHEP* **10** (2010) 045 [arXiv:1003.3232] [INSPIRE].

[15] Z.-W. Chong, H. Lü and C. Pope, *BPS geometries and AdS bubbles*, *Phys. Lett.* **B 614** (2005) 96 [hep-th/0412221] [INSPIRE].

[16] J.T. Liu, H. Lü, C. Pope and J.F. Vazquez-Poritz, *Bubbling AdS black holes*, *JHEP* **10** (2007) 030 [hep-th/0703184] [INSPIRE].

[17] B. Chen, S. Cremonini, A. Donos, F.-L. Lin, H. Lin, et al., *Bubbling AdS and droplet descriptions of BPS geometries in IIB supergravity*, *JHEP* **10** (2007) 003 [arXiv:0704.2233] [INSPIRE].

[18] J.B. Gutowski and H.S. Reall, *General supersymmetric AdS_5 black holes*, *JHEP* **04** (2004) 048 [hep-th/0401129] [INSPIRE].

[19] J.B. Gutowski and H.S. Reall, *Supersymmetric AdS_5 black holes*, *JHEP* **02** (2004) 006 [hep-th/0401042] [INSPIRE].

[20] H.K. Kunduri, J. Lucietti and H.S. Reall, *Supersymmetric multi-charge AdS_5 black holes*, *JHEP* **04** (2006) 036 [hep-th/0601156] [INSPIRE].

[21] J. Fernandez-Gracia and B. Fiol, *A no-hair theorem for extremal black branes*, *JHEP* **11** (2009) 054 [arXiv:0906.2353] [INSPIRE].

[22] V.E. Hubeny and M. Rangamani, *Unstable horizons*, *JHEP* **05** (2002) 027 [hep-th/0202189] [INSPIRE].

[23] S.S. Gubser and I. Mitra, *Instability of charged black holes in Anti-de Sitter space*, hep-th/0009126 [INSPIRE].

[24] S.S. Gubser and I. Mitra, *The evolution of unstable black holes in Anti-de Sitter space*, *JHEP* **08** (2001) 018 [hep-th/0011127] [INSPIRE].

[25] E. Gava, G. Milanesi, K. Narain and M. O'Loughlin, *1/8 BPS states in AdS/CFT*, *JHEP* **05** (2007) 030 [hep-th/0611065] [INSPIRE].

[26] M. Cvetič, H. Lü, C. Pope, A. Sadrzadeh and T.A. Tran, *Consistent* SO(6) *reduction of type IIB supergravity on S^5*, *Nucl. Phys.* **B 586** (2000) 275 [hep-th/0003103] [INSPIRE].

[27] J.T. Liu, H. Lü, C. Pope and J.F. Vazquez-Poritz, *New supersymmetric solutions of $N = 2$, $D = 5$ gauged supergravity with hyperscalars*, *JHEP* **10** (2007) 093 [arXiv:0705.2234] [INSPIRE].

[28] K. Behrndt, A.H. Chamseddine and W. Sabra, *BPS black holes in $N = 2$ five-dimensional AdS supergravity*, *Phys. Lett.* **B 442** (1998) 97 [hep-th/9807187] [INSPIRE].

[29] J.M. Heinzle, N. Rohr and C. Uggla, *Spherically symmetric relativistic stellar structures*, *Class. Quant. Grav.* **20** (2003) 4567 [gr-qc/0304012] [INSPIRE].

[30] V. Vaganov, *Self-gravitating radiation in AdS(d)*, arXiv:0707.0864 [INSPIRE].

JHEP11(2011)035

[31] J. Hammersley, *A critical dimension for the stability of radiating perfect fluid stars*, arXiv:0707.0961 [INSPIRE].

[32] R.D. Sorkin, R.M. Wald and Z.J. Zhang, *Entropy of selfgravitating radiation*, *Gen. Rel. Grav.* **13** (1981) 1127 [INSPIRE].

[33] D.N. Page and K. Phillips, *Selfgravitating radiation in Anti-de Sitter space*, *Gen. Rel. Grav.* **17** (1985) 1029 [INSPIRE].

[34] V.E. Hubeny, H. Liu and M. Rangamani, *Bulk-cone singularities and signatures of horizon formation in AdS/CFT*, *JHEP* **01** (2007) 009 [hep-th/0610041] [INSPIRE].

[35] F. Schunck and E. Mielke, *General relativistic boson stars*, *Class. Quant. Grav.* **20** (2003) R301 [arXiv:0801.0307] [INSPIRE].

[36] C.P. Herzog, *An analytic holographic superconductor*, *Phys. Rev.* **D 81** (2010) 126009 [arXiv:1003.3278] [INSPIRE].

[37] H. Lin, O. Lunin and J.M. Maldacena, *Bubbling AdS space and* 1/2 *BPS geometries*, *JHEP* **10** (2004) 025 [hep-th/0409174] [INSPIRE].

JHEP11(2011)035